Introduction to Synchrotron Radiation

David Attwood
University of California, Berkeley

The short wavelength region of the electromagnetic spectrum

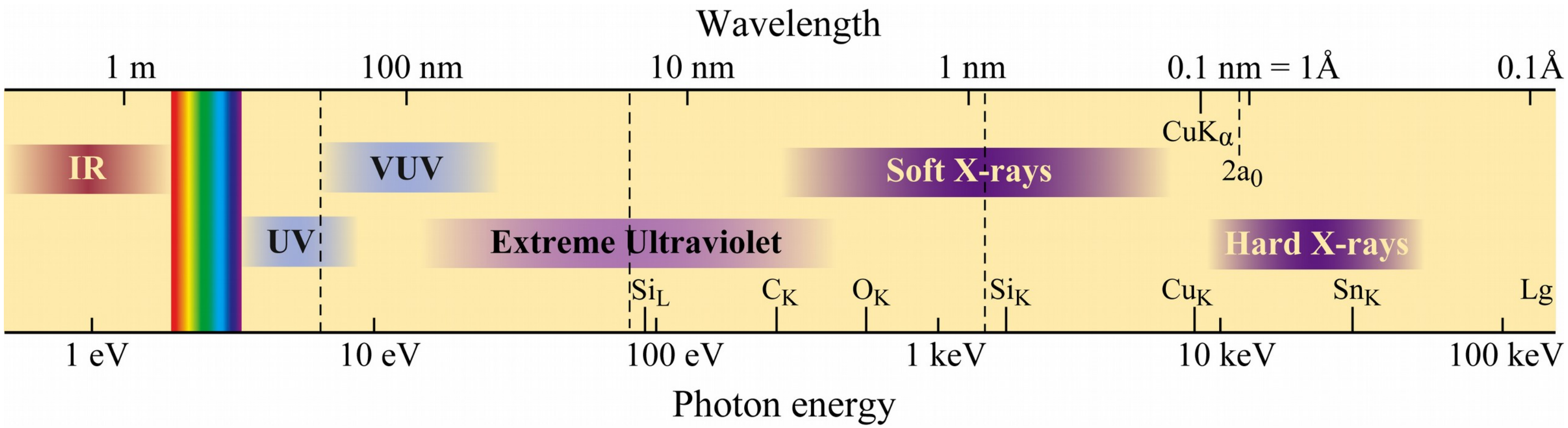

- Elemental and chemical sensitivity
- Penetrate visibly opaque objects
- See smaller features
- Write smaller patterns

Ch 01 F01 Feb2017 LG.ai

$$\hbar\omega \cdot \lambda = hc = 1239.842 \text{ eV nm}$$

$$n = 1 - \delta + i\beta \qquad \delta, \beta << 1$$

Broadly tunable radiation is needed to probe the primary (n = 1 & n = 2) resonances of the elements

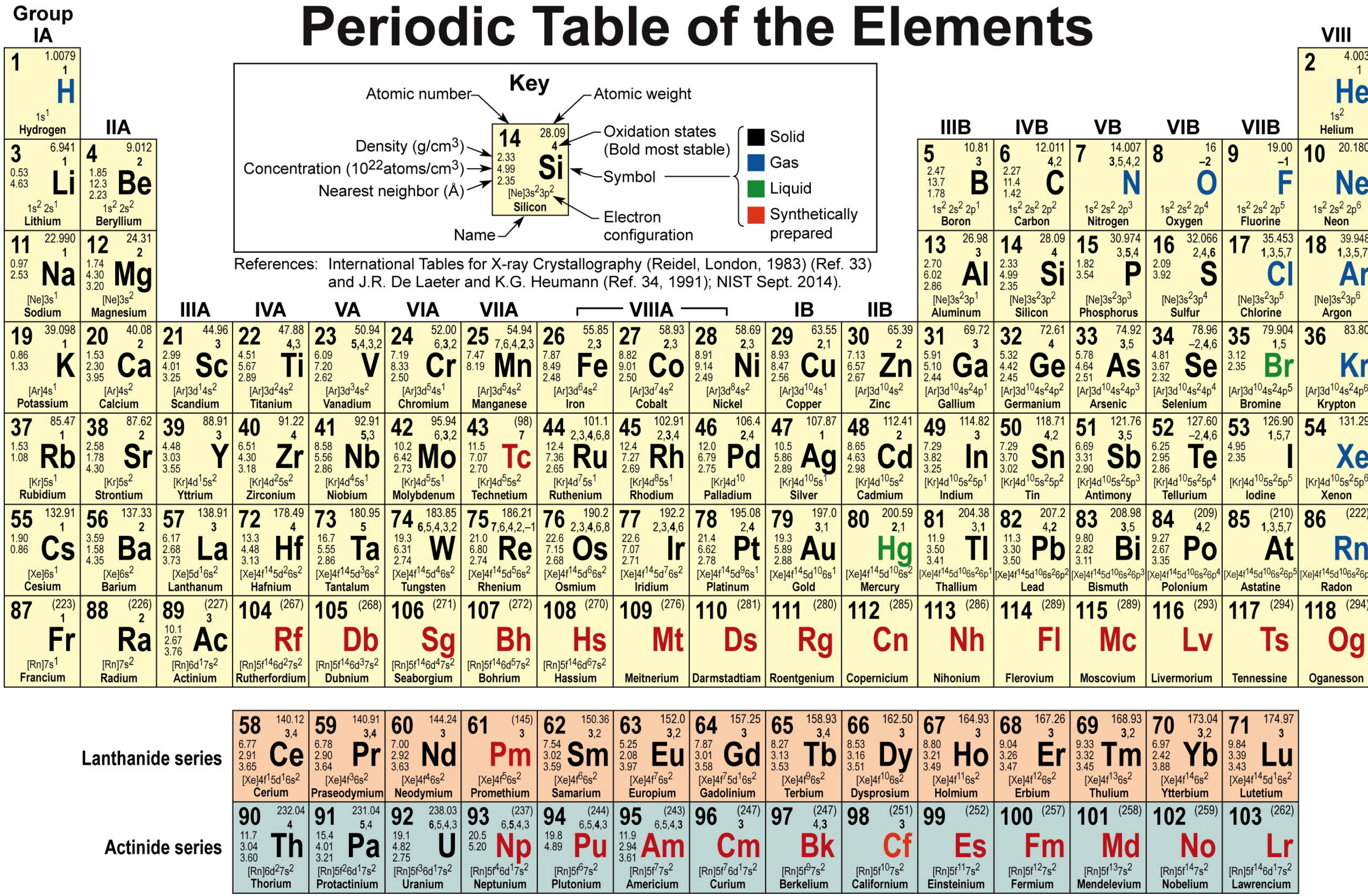

Electron binding energies, in electron volts (eV), for the elements in their natural forms

Element	K 1 s	L_1 2s	L_2 $2p_{1/2}$	L_3 $2p_{3/2}$	M_1 3s	M_2 $3p_{1/2}$	M_3 $3p_{3/2}$	M_4 $3d_{3/2}$	M_5 $3d_{5/2}$	N_1 4s	N_2 $4p_{1/2}$	N_3 $4p_{3/2}$
1 H	13.6											
2 He	24.6[b]											
3 Li	54.7[b]											
4 Be	111.5[b]											
5 B	188[b]											
6 C	284.2[b]											
7 N	409.9[b]	37.3[b]										
8 O	543.1[b]	41.6[b]										
9 F	696.7[b]											
10 Ne	870.2[b]	48.5[b]	21.7[b]	21.6[b]								
11 Na	1070.8[c]	63.5[c]	30.4[c]	30.5[b]								
12 Mg	1303.0[c]	88.6[b]	49.6[c]	49.2[c]								
13 Al	1559.6	117.8[b]	72.9[b]	72.5[b]								
14 Si	1838.9	149.7[b]	99.8[b]	99.2[b]								
15 P	2145.5	189[b]	136[b]	135[b]								
16 S	2472	230.9[b]	163.6[b]	162.5[b]								
17 Cl	2822.4	270.2[b]	202[b]	200[b]								
18 Ar	3205.9[b]	326.3[b]	250.6[b]	248.4[b]	29.3[b]	15.9[b]	15.7[b]					
19 K	3608.4[b]	378.6[b]	297.3[b]	294.6[b]	34.8[b]	18.3[b]	18.3[b]					
20 Ca	4038.5[b]	438.4[c]	349.7[c]	346.2[c]	44.3 [c]	25.4[c]	25.4[c]					
21 Sc	4492.8	498.0[b]	403.6[b]	398.7[b]	51.1[b]	28.3[b]	28.3[b]					
22 Ti	4966.4	560.9[c]	461.2[c]	453.8[c]	58.7[c]	32.6[c]	32.6[c]					
23 V	5465.1	626.7[c]	519.8[c]	512.1[c]	66.3[c]	37.2[c]	37.2[c]					
24 Cr	5989.2	695.7[c]	583.8[c]	574.1[c]	74.1[c]	42.2[c]	42.2[c]					
25 Mn	6539.0	769.1[c]	649.9[c]	638.7[c]	82.3[c]	47.2[c]	47.2[c]					
26 Fe	7112.0	844.6[c]	719.9[c]	706.8[c]	91.3[c]	52.7[c]	52.7[c]					
27 Co	7708.9	925.1[c]	793.3[c]	778.1[c]	101.0[c]	58.9[c]	58.9[c]					
28 Ni	8332.8	1008.6[c]	870.0[c]	852.7[c]	110.8[c]	68.0[c]	66.2[c]					
29 Cu	8978.9	1096.7[c]	952.3[c]	932.5[c]	122.5[c]	77.3[c]	75.1[c]					
30 Zn	9658.6	1196.2[b]	1044.9[b]	1021.8[b]	139.8[b]	91.4[b]	88.6[b]	10.2[b]	10.1[b]			
31 Ga	10367.1	1299.0[b]	1143.2[c]	1116.4[c]	159.5[c]	103.5[c]	103.5[c]	18.7[c]	18.7[c]			
32 Ge	11103.1	1414.6[b]	1248.1[b]	1217.0[b]	180.1[b]	124.9[b]	120.8[b]	29.0[b]	29.0[b]			
33 As	11866.7	1527.0[b]	1359.1[b]	1323.6[b]	204.7[b]	146.2[b]	141.2[b]	41.7[b]	41.7[b]			
34 Se	12657.8	1652.0[b]	1474.3[b]	1433.9[b]	229.6[b]	166.5[b]	160.7[b]	55.5[b]	54.6[b]			
35 Br	13473.7	1782.0[b]	1596.0[b]	1549.9[b]	257[b]	189[b]	182[b]	70[b]	69[b]			
36 Kr	14325.6	1921.0	1730.9[b]	1678.4[b]	292.8[b]	222.2[b]	214.4	95.0[b]	93.8[b]	27.5[b]	14.1[b]	14.1[b]
37 Rb	15199.7	2065.1	1863.9	1804.4	326.7[b]	248.7[b]	239.1[b]	113.0[b]	112[b]	30.5[b]	16.3[b]	15.3 [b]
38 Sr	16104.6	2216.3	2006.8	1939.6	358.7[c]	280 3[c]	270.0[c]	136.0[c]	134.2[c]	38.9[c]	20.3[c]	20.3[c]
39 Y	17038.4	2372.5	2155.5	2080.0	392.0[b]	310.6[b]	298.8[b]	157.7[c]	155.8[c]	43.8[b]	24.4[b]	23.1[b]
40 Zr	17997.6	2531.6	2306.7	2222.3	430.3[c]	343.5[c]	329.8[c]	181.1[c]	178.8[c]	50.6[c]	28.5[c]	27.7[c]
41 Nb	18985.6	2697.7	2464.7	2370.5	466.6[c]	376.1[c]	360.6[c]	205.0[c]	202.3[c]	56.4[c]	32.6[c]	30.8[c]
42 Mo	19999.5	2865.5	2625.1	2520.2	506.3[c]	411.6[c]	394.0[c]	231.1[c]	227.9[c]	63.2[c]	37.6[c]	35.5[c]
43 Tc	21044.0	3042.5	2793.2	2676.9	544[b]	445[b]	425[b]	257[b]	253[b]	68[b]	39[c]	39[b]
44 Ru	22117.2	3224.0	2966.9	2837.9	586.2[c]	483.5[c]	461.4[c]	284.2[c]	280.0[c]	75.0[c]	46.5[c]	43.2[c]
45 Rh	23219.9	3411.9	3146.1	3003.8	628.1[c]	521.3[c]	496.5[c]	311.9[c]	307.2[c]	81.4[b]	50.5[c]	47.3[c]
46 Pd	24350.3	3604.3	3330.3	3173.3	671.6[c]	559.9[c]	532.3[c]	340.5[c]	335.2 [c]	87.6[b]	55.7[c]	50.9[c]
47 Ag	25514.0	3805.8	3523.7	3351.1	719.0[c]	603.8[c]	573.0[c]	374.0[c]	368.0[c]	97.0[c]	63.7[c]	58.3[c]

www.cxro.lbl.gov

ApxB_1_47.ai

Synchrotron radiation

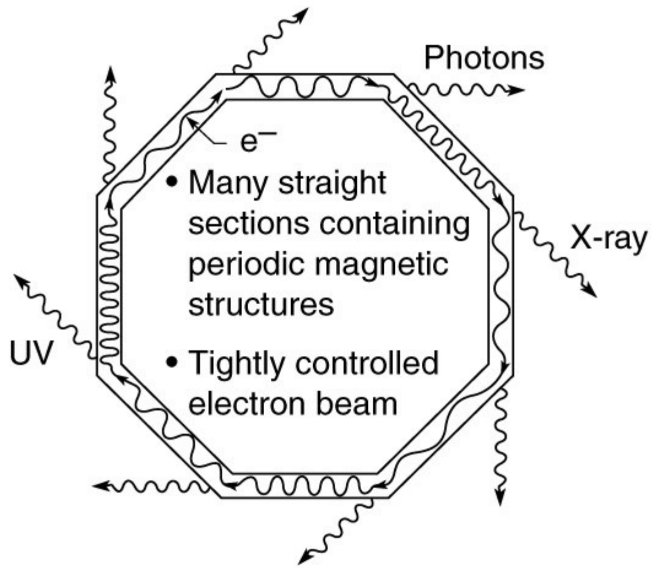

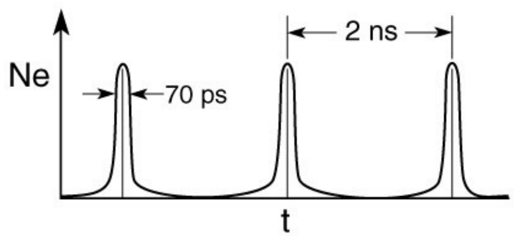

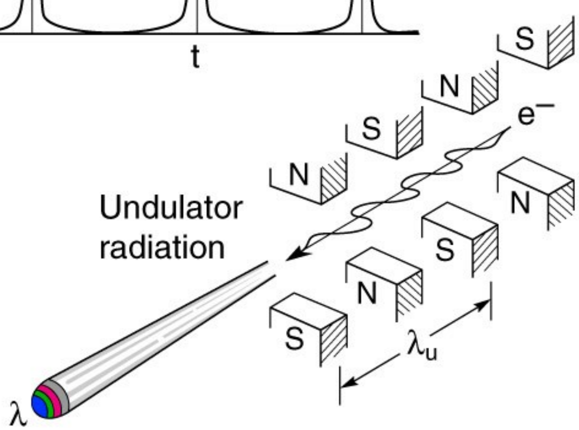

Bending Magnet:

$$\hbar\omega_c = \frac{3e\hbar B\gamma^2}{2m} \qquad (5.7)$$

Wiggler:

$$\hbar\omega_c = \frac{3e\hbar B\gamma^2}{2m} \qquad (5.80)$$

$$n_c = \frac{3K}{4}\left(1 + \frac{K^2}{2}\right) \qquad (5.82)$$

$$P_T = \frac{\pi e K^2\gamma^2 I N}{3\epsilon_0\lambda_u} \qquad (5.85)$$

Undulator:

$$\lambda = \frac{\lambda_u}{2\gamma^2}\left(1 + \frac{K^2}{2} + \gamma^2\theta^2\right) \qquad (5.28)$$

$$K = \frac{eB_0\lambda_u}{2\pi mc} \qquad (5.18)$$

$$\theta_{cen} = \frac{1}{\gamma^*\sqrt{N}} \qquad (5.15)$$

$$\left.\frac{\Delta\lambda}{\lambda}\right|_{cen} = \frac{1}{N} \qquad (5.14)$$

$$\bar{P}_{cen} = \frac{\pi e\gamma^2 I}{\epsilon_0\lambda_u}\frac{K^2}{\left(1+\frac{K^2}{2}\right)^2}[JJ]^2 \qquad (5.41)$$

Ch05_F00VG_Jan06.ai

Synchrotron radiation from relativistic electrons

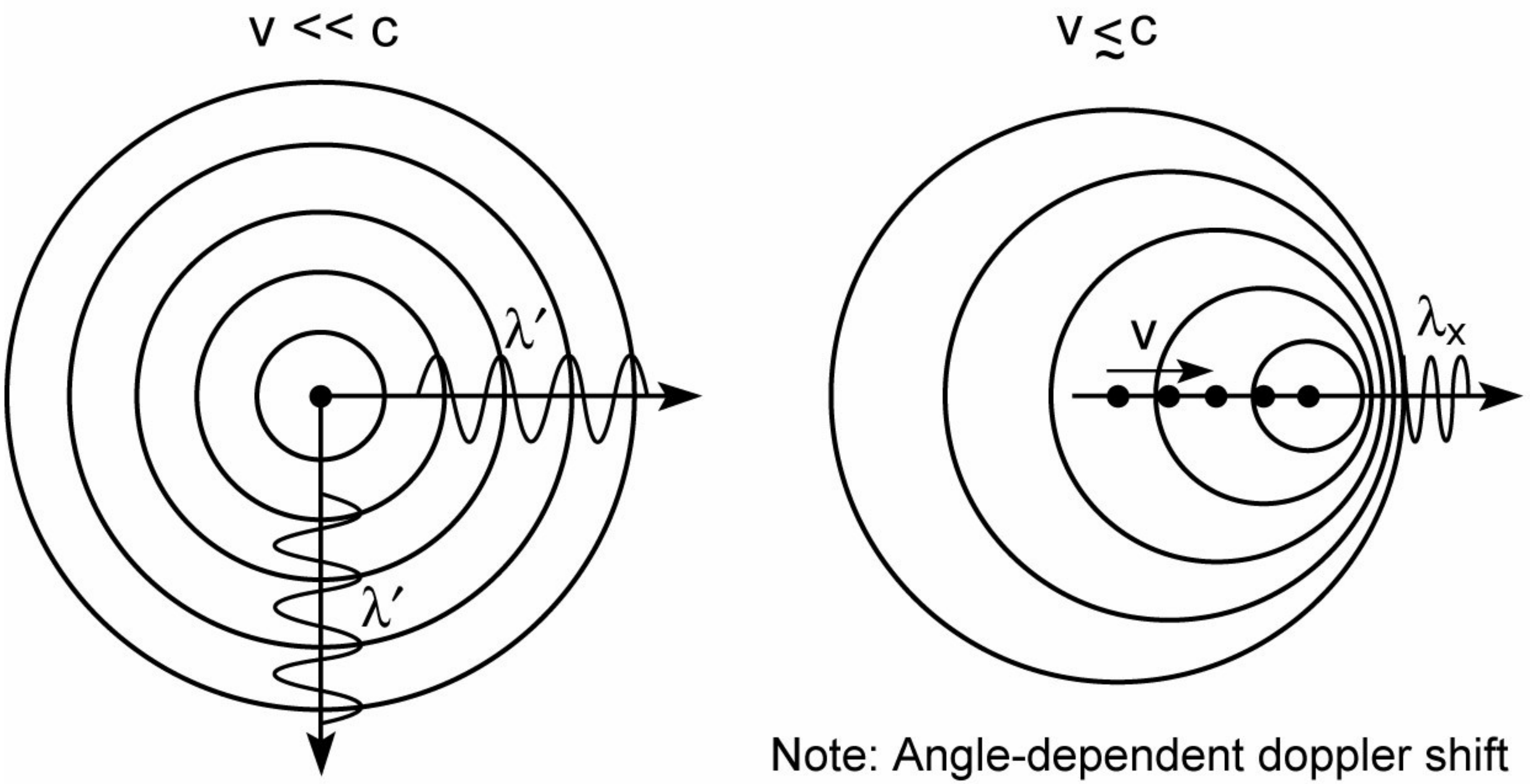

Note: Angle-dependent doppler shift

$$\lambda = \lambda' \left(1 - \frac{v}{c}\cos\theta\right) \qquad \lambda = \lambda' \gamma \left(1 - \frac{v}{c}\cos\theta\right)$$

$$\gamma = \frac{1}{\sqrt{1 - \frac{v^2}{c^2}}}$$

Following John Madey

Ch05_F09VG_revOct05.ai

Undulator radiation from a small electron beam radiating into a narrow forward cone is very bright

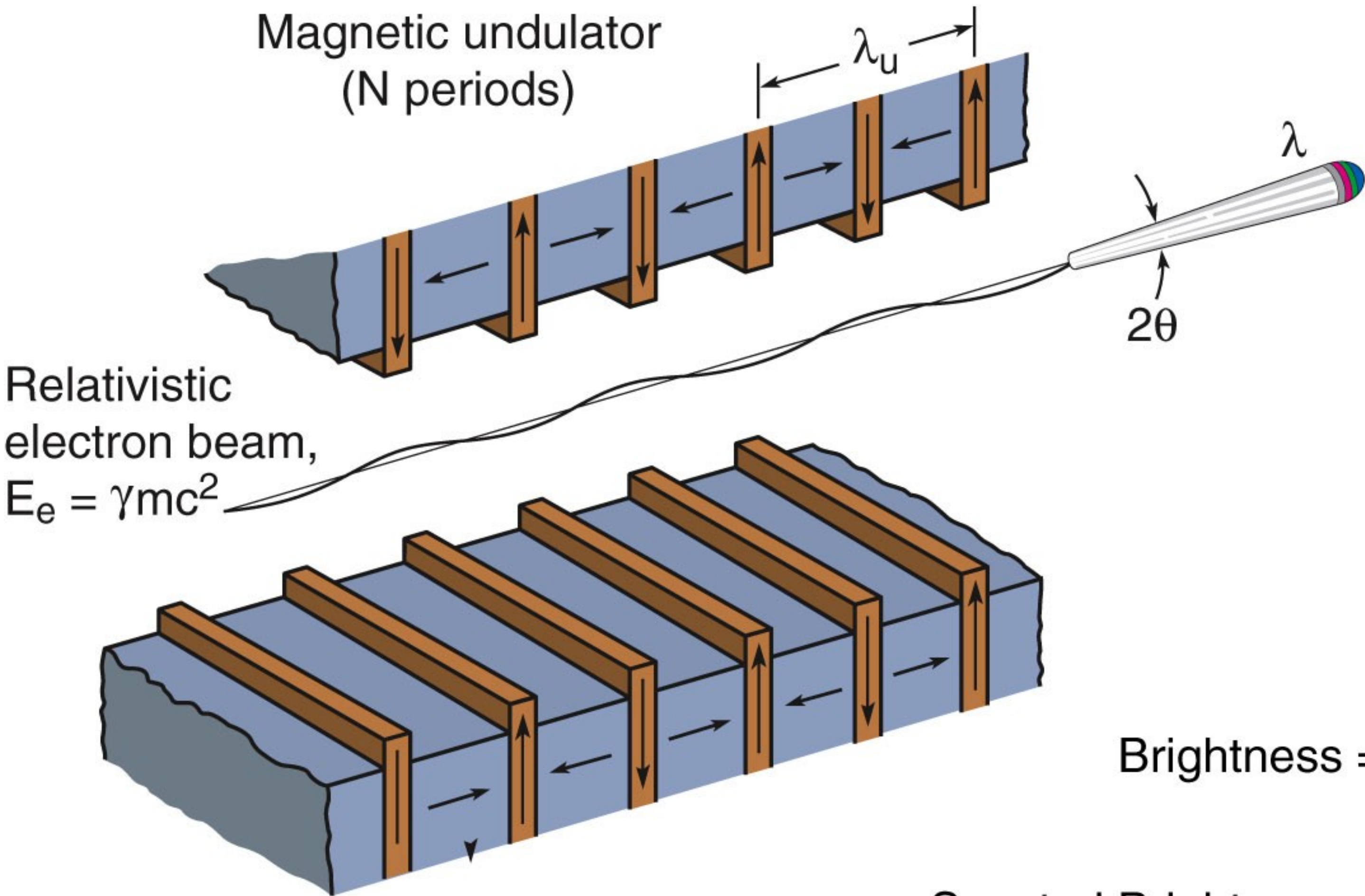

$$\lambda \simeq \frac{\lambda_u}{2\gamma^2}$$

$$\theta_{cen} \simeq \frac{1}{\gamma\sqrt{N}}$$

$$\left[\frac{\Delta\lambda}{\lambda}\right]_{cen} = \frac{1}{N}$$

$$\text{Brightness} = \frac{\text{photon flux}}{(\Delta A)\,(\Delta\Omega)}$$

$$\text{Spectral Brightness} = \frac{\text{photon flux}}{(\Delta A)\,(\Delta\Omega)\,(\Delta\lambda/\lambda)}$$

Ch05_F08VG_1.04.ai

Undulator radiation

Laboratory Frame of Reference	Frame of Moving e⁻	Frame of Observer	Following Monochromator

Laboratory Frame of Reference

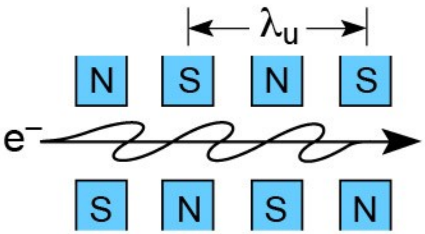

$E = \gamma mc^2$

$$\gamma = \frac{1}{\sqrt{1 - \frac{v^2}{c^2}}}$$

N = # periods

Frame of Moving e⁻

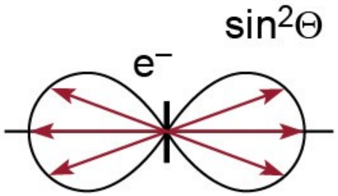

e⁻ radiates at the Lorentz contracted wavelength:

$$\lambda' = \frac{\lambda_u}{\gamma}$$

Bandwidth:

$$\frac{\lambda'}{\Delta\lambda'} \simeq N$$

Frame of Observer

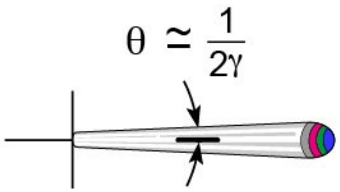

Doppler shortened wavelength on axis:

$$\lambda = \lambda'\gamma(1 - \beta\cos\theta)$$

$$\lambda = \frac{\lambda_u}{2\gamma^2}(1 + \gamma^2\theta^2)$$

Accounting for transverse motion due to the periodic magnetic field:

$$\lambda = \frac{\lambda_u}{2\gamma^2}\left(1 + \frac{K^2}{2} + \gamma^2\theta^2\right)$$

where $K = eB_0\lambda_u/2\pi mc$

Following Monochromator

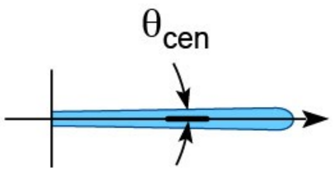

For $\frac{\Delta\lambda}{\lambda} \simeq \frac{1}{N}$

$$\theta_{cen} \simeq \frac{1}{\gamma\sqrt{N}}$$

typically

$\theta_{cen} \simeq$ 10-30 μrad

Ch05_LG186_June2014.ai

Calculating Power in the Central Radiation Cone: Using the well known "dipole radiation" formula by transforming to the frame of reference moving with the electrons

x, z, t laboratory frame of reference

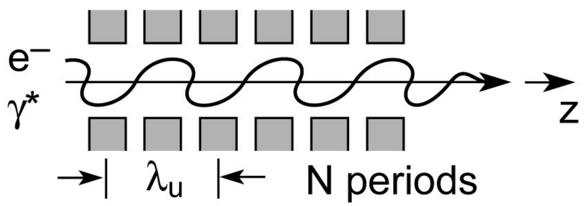

Lorentz transformation

x', z', t' frame of reference moving with the average velocity of the electron

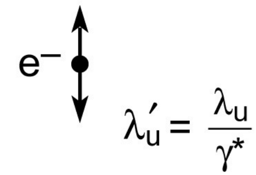

Determine *x, z, t* motion:

$$\frac{d\mathbf{p}}{dt} = -e\,(\mathbf{E} + \mathbf{v} \times \mathbf{B})$$

Dipole radiation:

$$\frac{dP'}{d\Omega'} = \frac{e^2 a'^2 \sin^2 \Theta'}{16\pi^2 \epsilon_0 c^3}$$

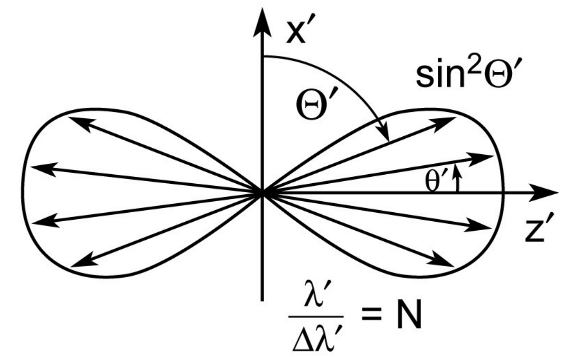

Lorentz transformation

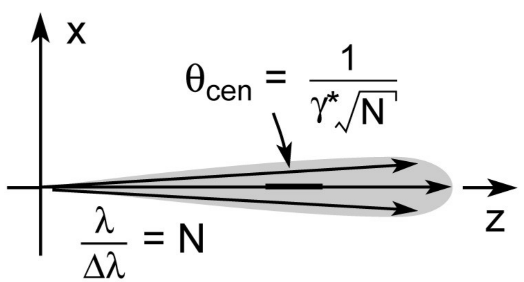

$$\bar{P}_{cen} = \frac{\pi e \gamma^2 I}{\epsilon_0 \lambda_u} \frac{K^2}{(1 + K^2/2)^2}$$

$$\frac{dP'}{d\Omega'} = \frac{e^2 c \gamma^2}{4\epsilon_0 \lambda_u^2} \frac{K^2}{(1 + K^2/2)^2} (1 - \sin^2 \theta' \cos^2 \phi') \cos^2 \omega'_u t'$$

Ch05_T4_Feb07.ai

Power in the central radiation cone

$$\lambda_x = \frac{\lambda_u}{2\gamma^2}\left(1 + \frac{K^2}{2} + \gamma^2\theta^2\right)$$

$$\bar{P}_{cen} = \frac{\pi e \gamma^2 I}{\epsilon_0 \lambda_u} \frac{K^2}{\left(1 + \frac{K^2}{2}\right)^2} [JJ]^2$$

$$\theta_{cen} = \frac{1}{\gamma^* \sqrt{N}}$$

$$\left(\frac{\Delta\lambda}{\lambda}\right)_{cen} = \frac{1}{N}$$

$$K = \frac{eB_0\lambda_u}{2\pi m_0 c}$$

$$\gamma^* = \gamma / \sqrt{1 + \frac{K^2}{2}}$$

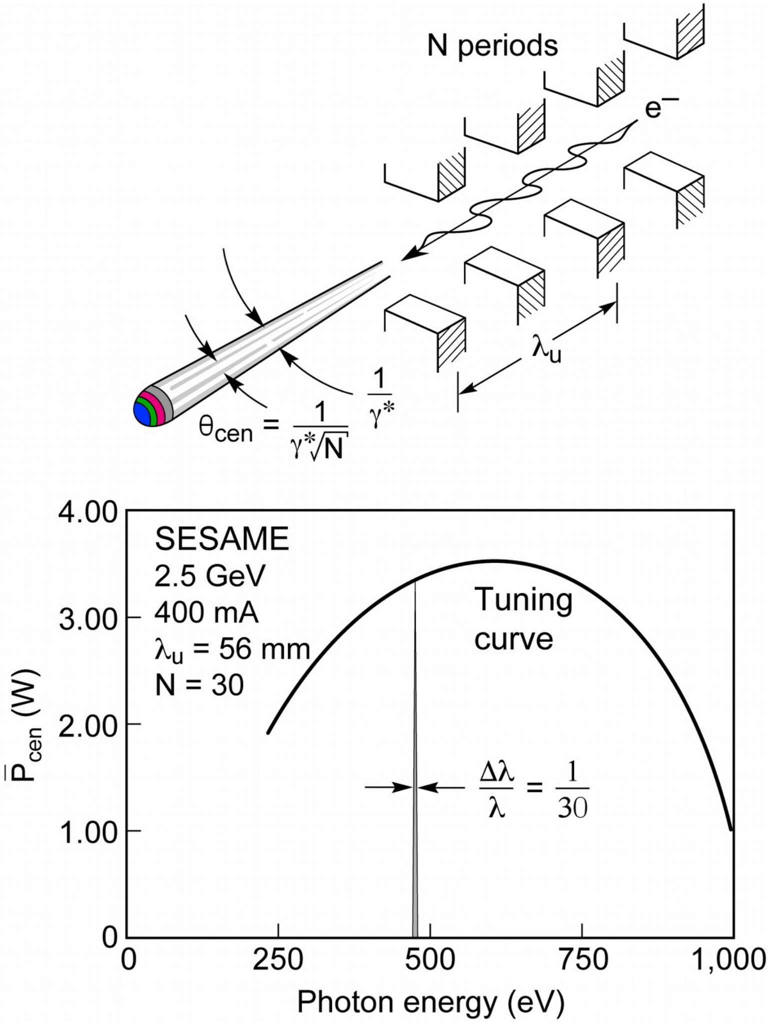

PowerCentralCone_SESAME.ai

APPLE II Elliptically Polarizing Undulator (EPU)

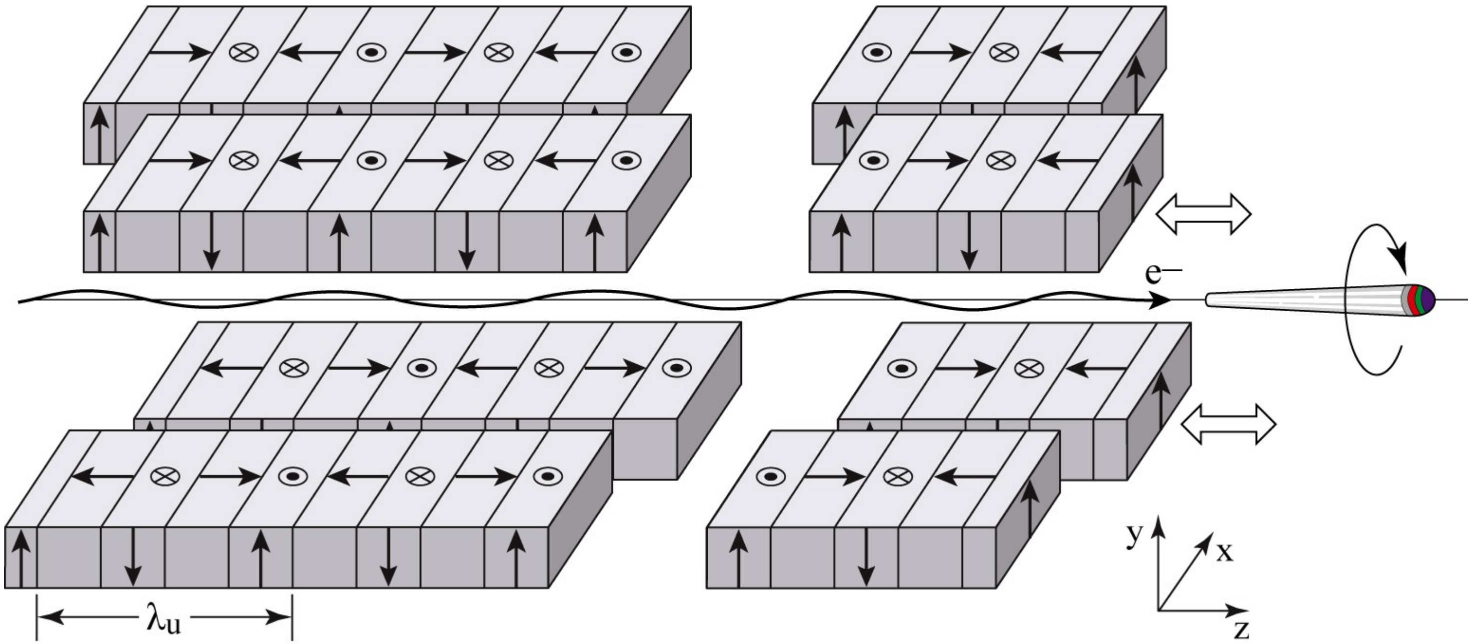

EPU at SESAME

Add Si, C, Fe to both

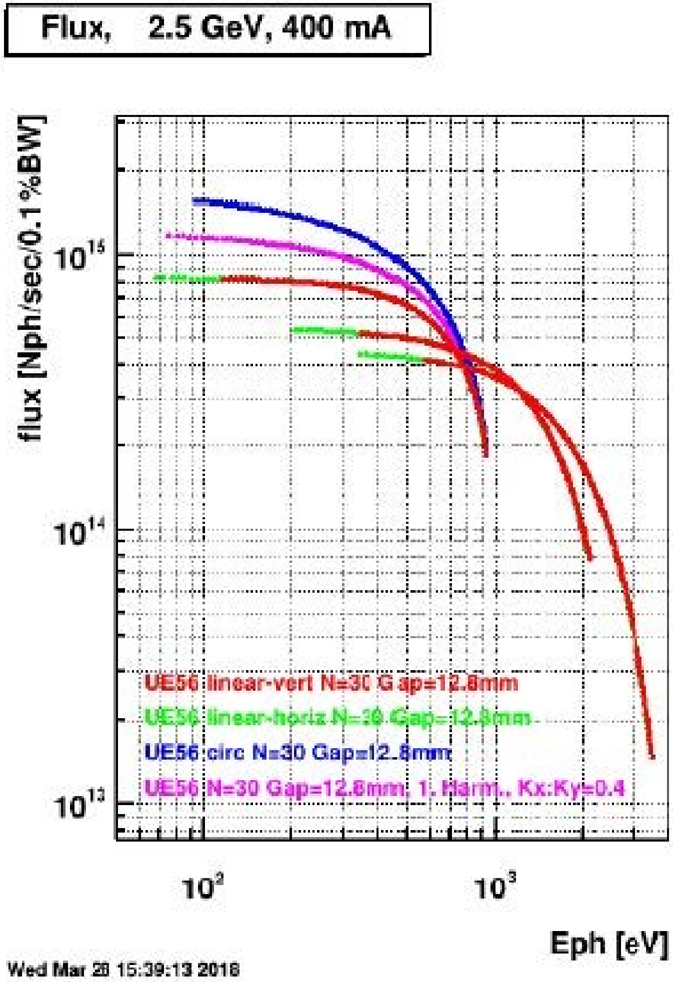

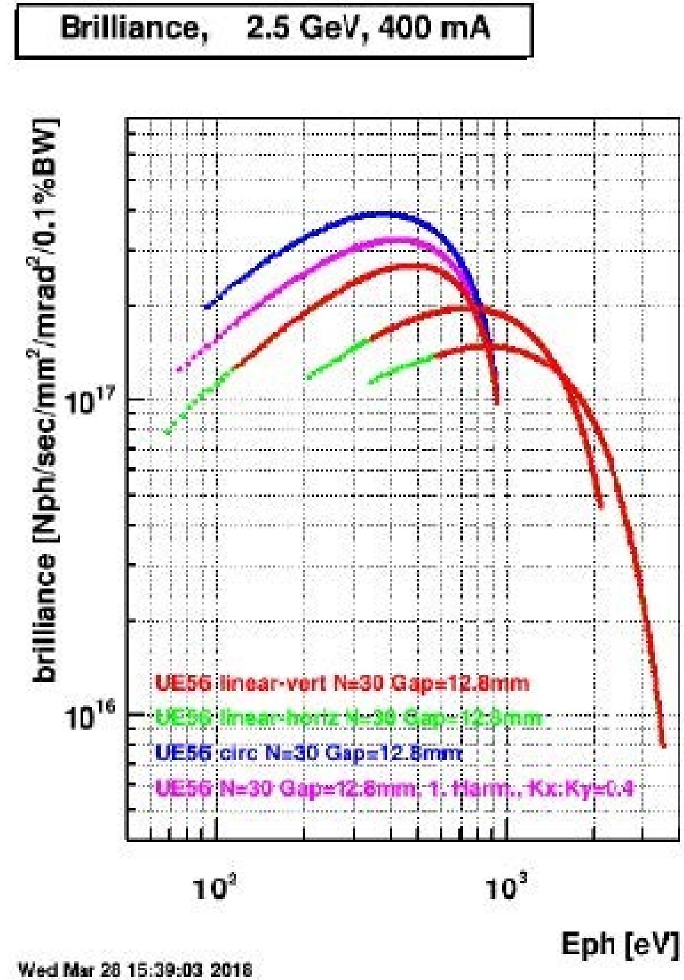

Bending magnet radiation covers a broad region of the spectrum, including the primary absorption edges of most elements

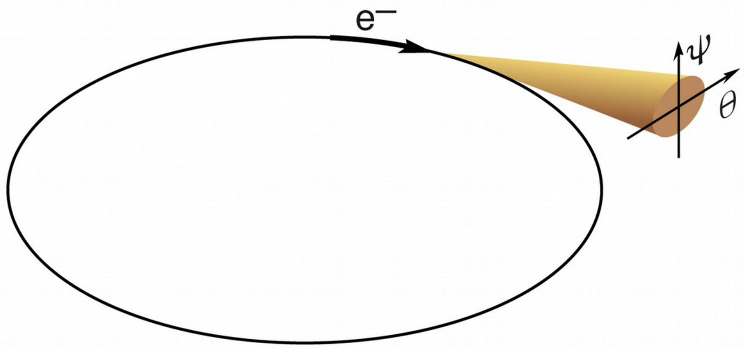

$$E_c = \hbar\omega c = \frac{3e\hbar\gamma^2}{2m} \qquad (5.7a)$$

$$E_c[\text{keV}] = 0.6650 E_e^2[\text{GeV}]B[\text{T}] \qquad (5.7b)$$

$$F_{1\text{mrad},\,0.1\%\text{BW}} = 2.46 \times 10^{13}\ \text{E}_e[\text{GeV}]\text{I}[\text{A}]\text{G}_1(\text{E}/\text{E}_c)\ \text{ph/sec} \qquad (5.8)$$

where $G_1(1) = 0.6514$

Advantages:
- covers broad spectral range
- least expensive
- most accessable

Disadvantages:
- not as bright as an undulator

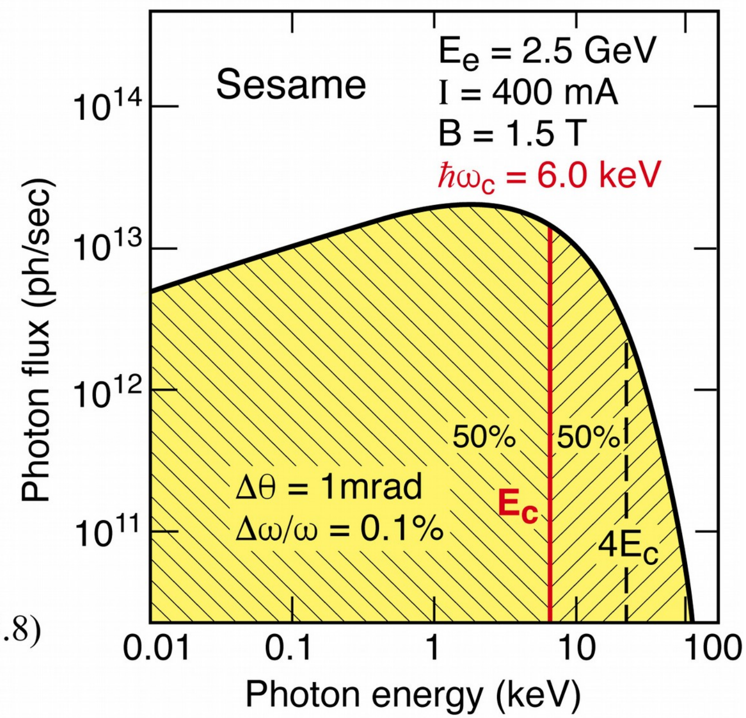

$E_c = 6$ keV

$4E_c = 24$ keV

Ch05_F07_Sesame.ai

A typical beamline: A monochromator plus glancing incidence optics deliver radiation to the sample

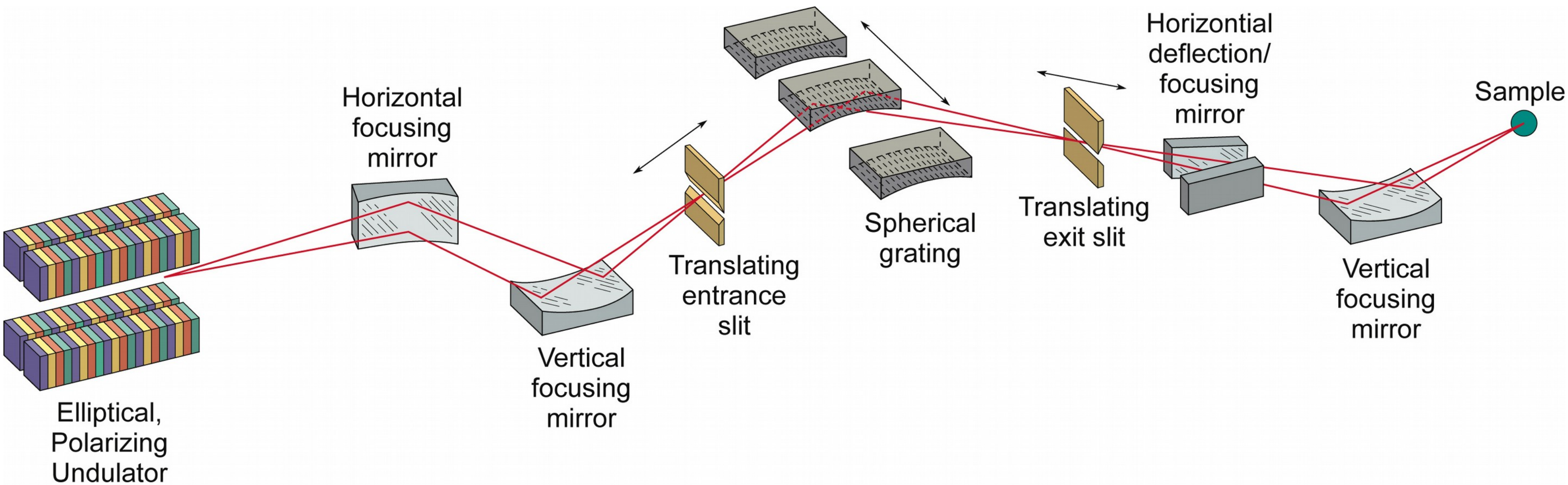

Available Optical Techniques for Soft X-Rays and EUV

- Reflection (glancing incidence or multilayer coatings)

- Diffraction (zone plates, gratings, pinholes)

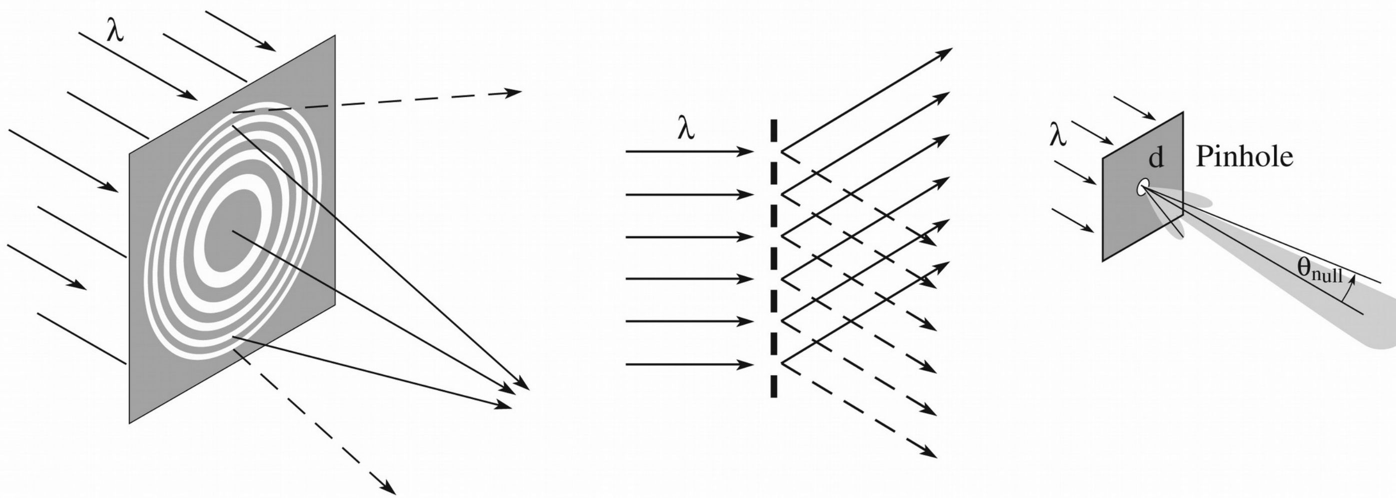

- Refraction (only for hard x-rays, > 20 keV)

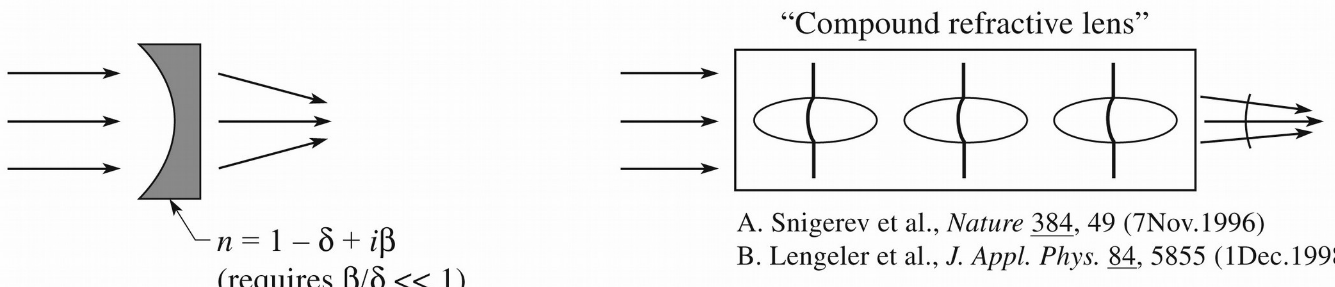

A. Snigerev et al., *Nature* 384, 49 (7Nov.1996)
B. Lengeler et al., *J. Appl. Phys.* 84, 5855 (1Dec.1998)

AvaiOpticTechSXREUV.ai

Refractive index at x-ray wavelengths

Based on a simple, semi-classical oscillator in the presence of an electric field $E = E_0 \cos\omega t$

$$n(\omega) = 1 - \frac{1}{2}\frac{e^2 n_a}{\epsilon_0 m}\sum_s \frac{g_s}{(\omega^2 - \omega_s^2) + i\gamma\omega} \qquad (3.8)$$

Expressed in terms of atomic scattering factors:

$$\boxed{n(\omega) = 1 - \frac{n_a r_e \lambda^2}{2\pi}\left[f_1^0(\omega) - i f_2^0(\omega)\right]} \qquad (3.9)$$

which we can write simply as

$$n(\omega) = 1 - \delta + i\beta \qquad (3.12)$$

Refractive index at nanometer wavelengths

Refractive Index

$$n = 1 - \delta + i\beta = 1 - \frac{n_a r_e \lambda^2}{2\pi}(f_1^{\,0} - i f_2^{\,0})$$

Atomic scattering factors

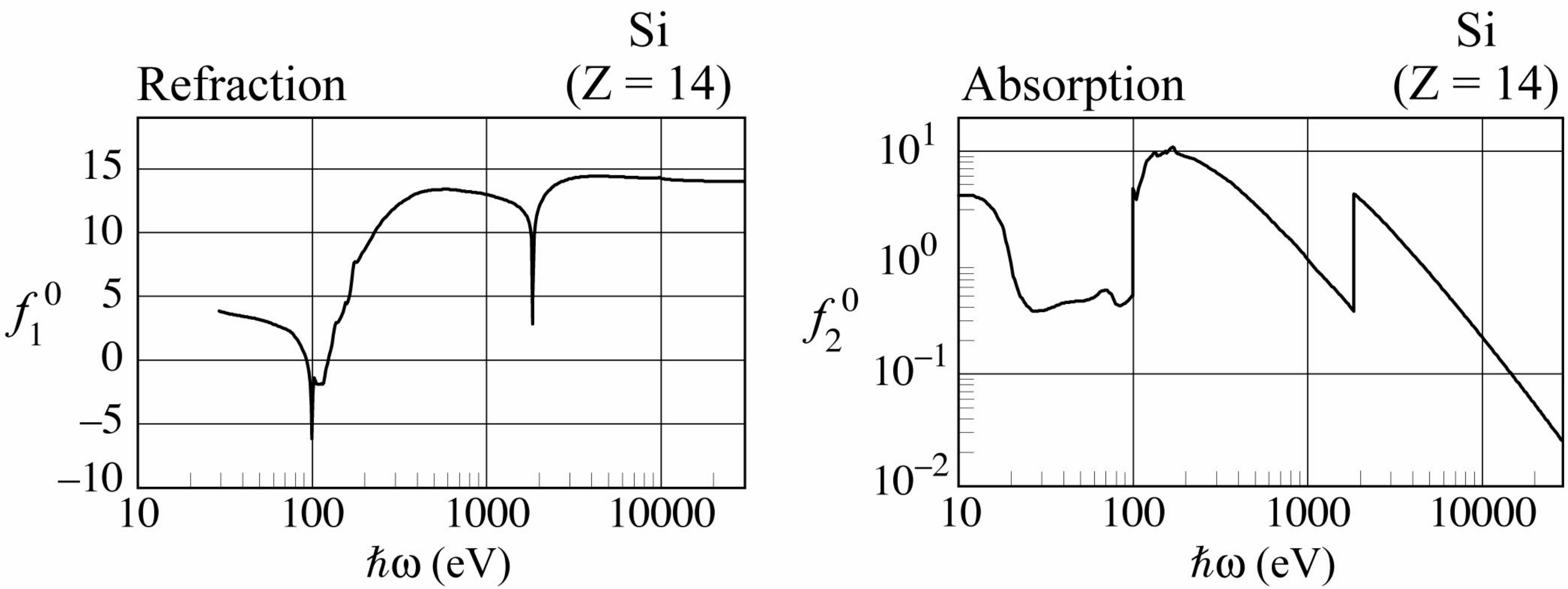

www.cxro.LBL.gov/optical_constants

ScattrngRefracIndex_June2009.ai

Refractive index from the IR to x-ray spectral region

$$n(\omega) = 1 - \delta + i\beta \quad (3.12)$$

$$\delta = \frac{n_a r_e \lambda^2}{2\pi} f_1^0(\omega) \quad (3.13a)$$

$$\beta = \frac{n_a r_e \lambda^2}{2\pi} f_2^0(\omega) \quad (3.13b)$$

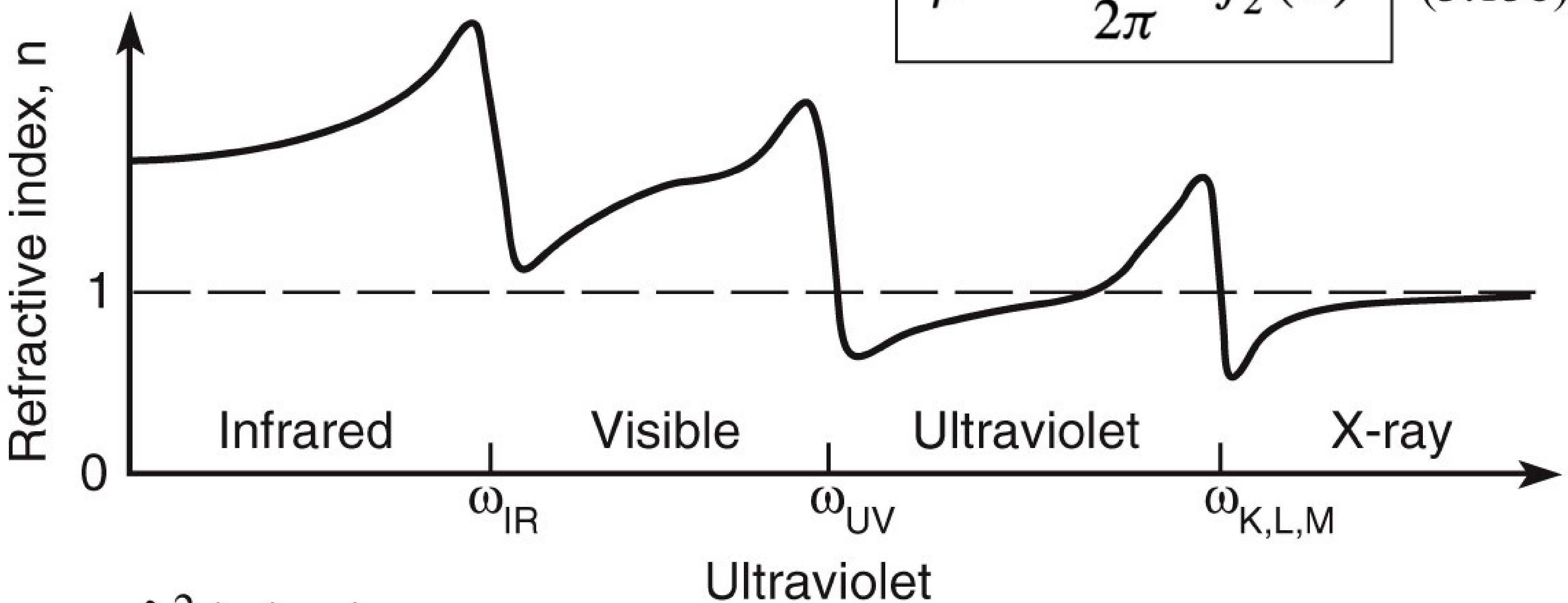

- λ^2 behavior
- δ & β << 1
- δ-crossover

Ch03_RefrcIndxIR.XR.ai

Normal incidence reflection of x-rays is very small

$$R_s = \frac{\left|\cos\phi - \sqrt{n^2 - \sin^2\phi}\right|^2}{\left|\cos\phi + \sqrt{n^2 - \sin^2\phi}\right|^2} \qquad (3.49)$$

at $\phi = 0$:

$$R_{s,\perp} = \frac{|1-n|^2}{|1+n|^2} = \frac{(1-n)(1-n^*)}{(1+n)(1+n^*)}$$

For $n = 1 - \delta + i\beta$

$$R_{s,\perp} = \frac{(\delta - i\beta)(\delta + i\beta)}{(2-\delta+i\beta)(2-\delta-i\beta)} = \frac{\delta^2+\beta^2}{(2-\delta)^2+\beta^2}$$

Reflectivity for x-ray and EUV radiation at normal incidence ($\phi = 0$):

$$R_{s,\perp} \simeq \frac{\delta^2+\beta^2}{4} \qquad (3.50)$$

Example: Nickel @ 300 eV (4.13 nm)
$f_1^\circ = 17.8$ $\quad f_2^\circ = 7.70$
$\delta = 0.0124$ $\quad \beta = 0.00538$

$R_\perp = 4.58 \times 10^{-5}$ [@ 300 eV]
[~ 10^{-8} at 3 keV]

Ch03_NormIncidReflc_5.05.ai

Glancing Incidence Optics

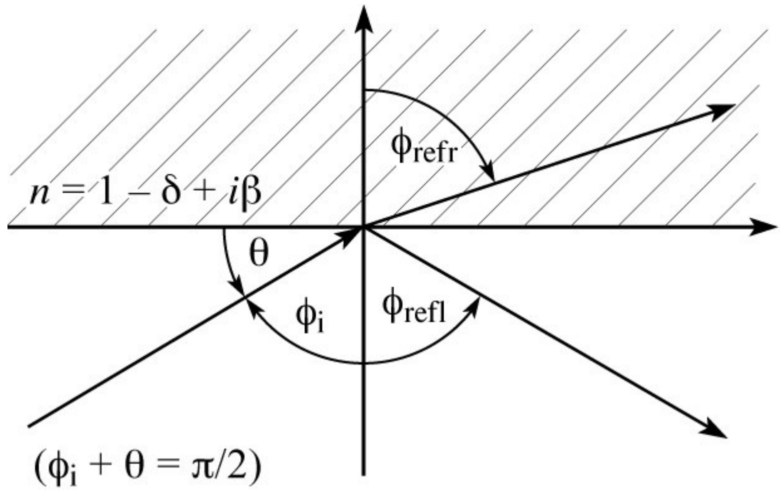

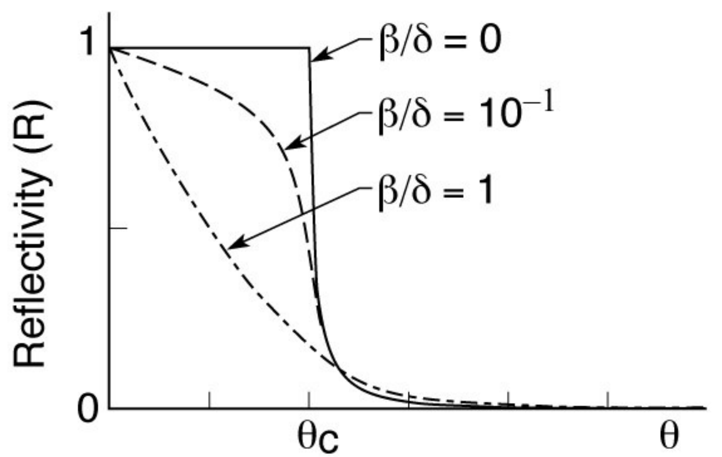

Snell's Law: $\text{Sin}\,\phi_{refr.} = \frac{\text{Sin}\,\phi_i}{n}$

Total external Reflection:

$$\phi_{refr.} \rightarrow \frac{\pi}{2} \text{ as } \phi_i \rightarrow \phi_{critical}$$

$$\text{Snell's Law: } 1 = \frac{\text{Sin}\,\phi_c}{1-\delta}$$

$$\text{Sin}(90^\circ - \theta_c) = 1 - \delta$$

$$\text{Cos}\,\theta_c = 1 - \delta$$

$$1 - \frac{\theta_c^2}{2} = 1 - \delta$$

$$\theta_c = \sqrt{2\delta}$$

For gold at 1 keV

$$\delta = 2.1 \times 10^{-3}$$

$$\theta_c = 3.7^\circ$$

(www.cxro.LBL.gov ;
"X-ray properties of the elements"
"X-ray interaction with matter")

GlancngIncidncOptics_Feb2010.ai

Kirkpatrick-Baez Mirror Pair

Orthogonal mirrors cancel astigmatism

Elliptical surfaces for point to point imaging

Glancing incidence coatings for broad band applications, multilayer coatings for fixed bandpass

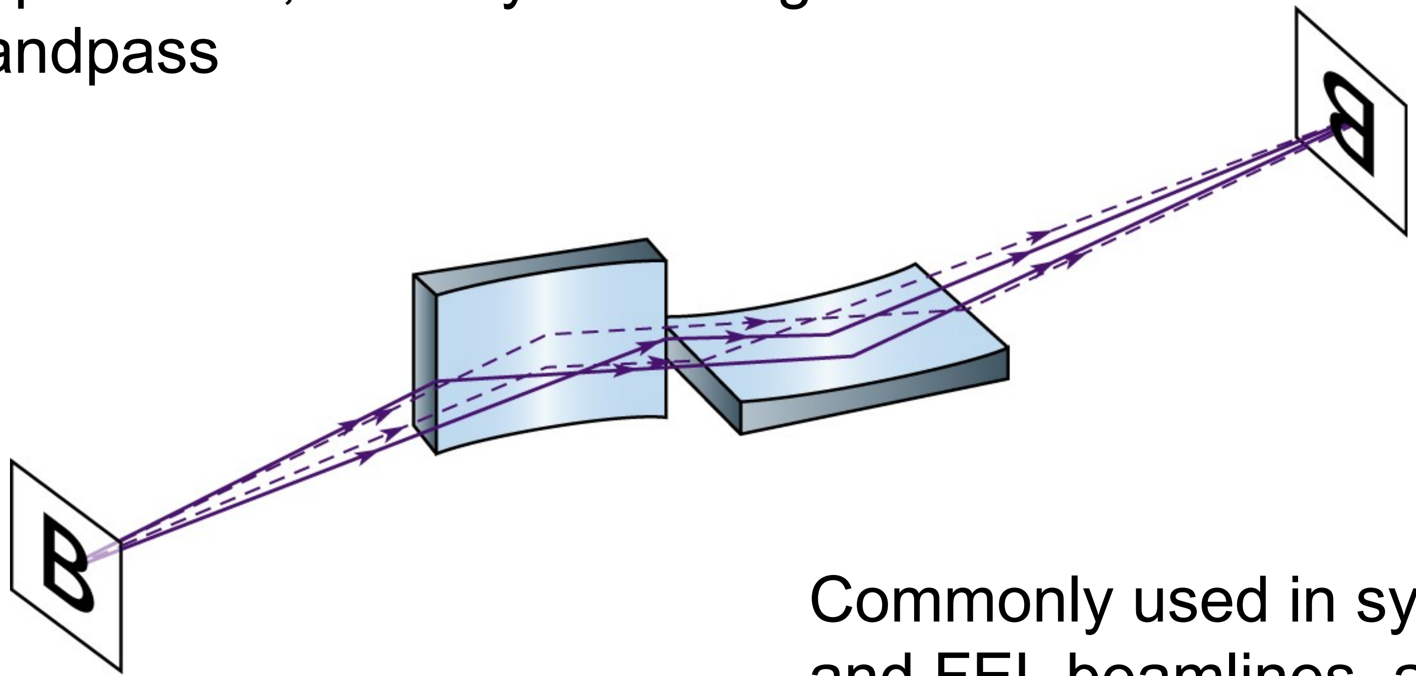

Courtesy of J. Underwood, LBNL

Commonly used in synchrotron and FEL beamlines, and in plasma diagnostics

X-ray microprobe at SPring-8

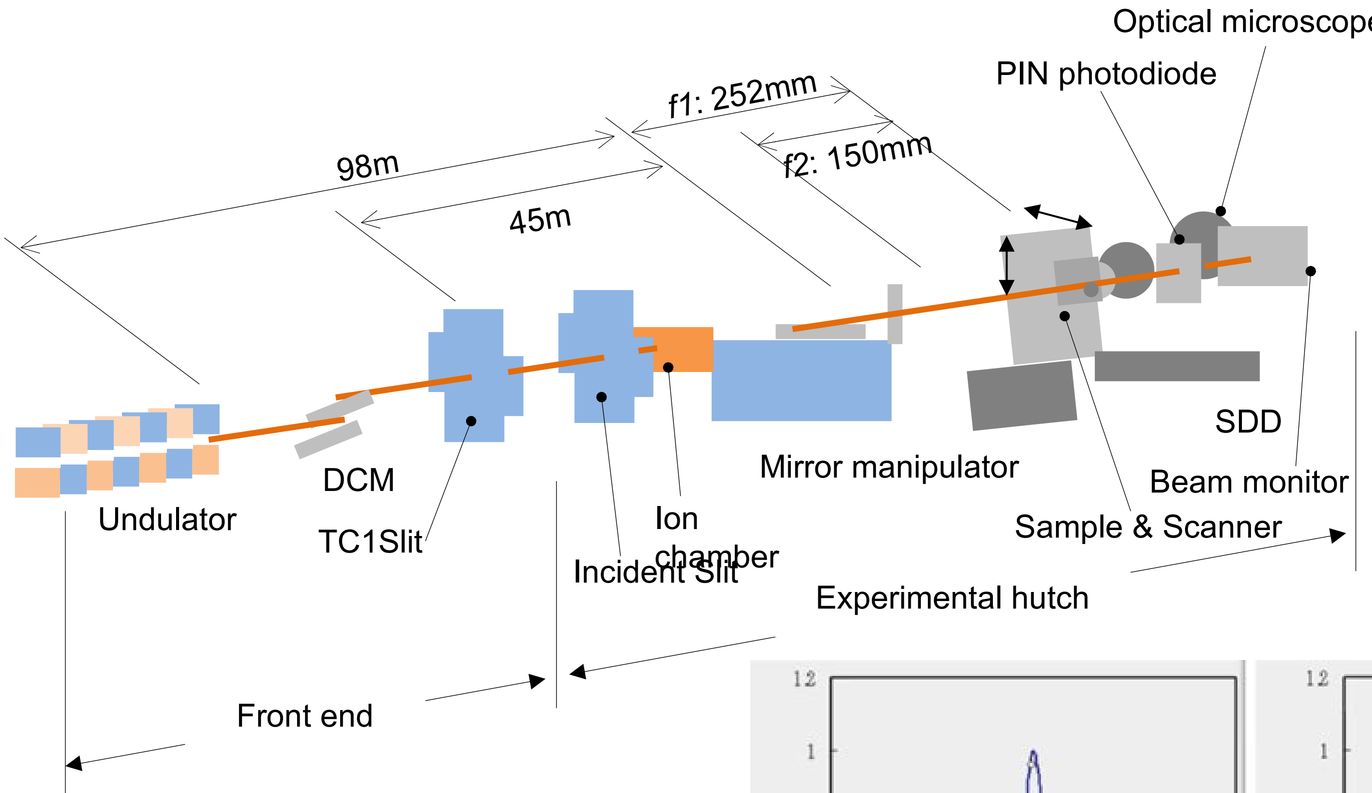

Now focused to 7 nm

S. Matsuyama et al., Rev. Sci. Instrum. 77, 103102 (2006)

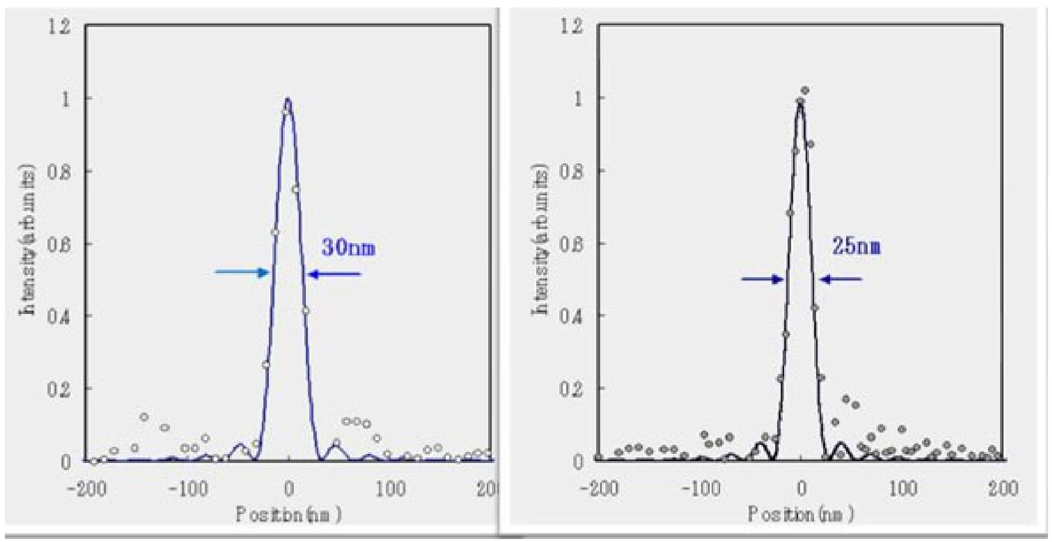

Courtesy of Professor Kazuto Yamauchi, Osaka University and Spring-8

Nested pairs of Wolter type 1 reflective x-ray optics for the orbiting Chandra X-ray Observatory

(a)

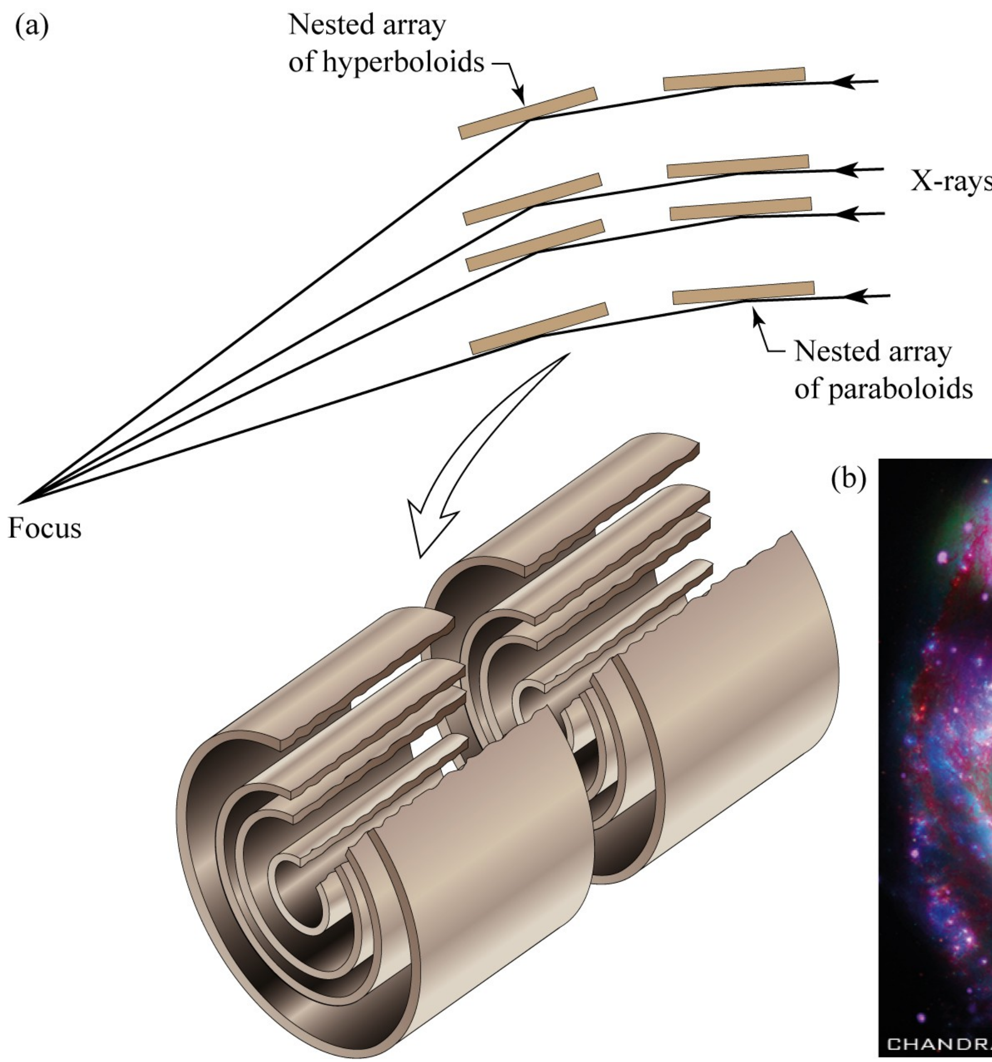

Composite view of the M51 "Whirlpool Galaxy"

(b)

Courtesy of D. Schwartz (Harvard-Smithsonian Center for Astrophysics) and NASA

Single surface mirrors for x-ray astronomy

Sharp cutoffs at 700 eV, 2 keV and 10 keV

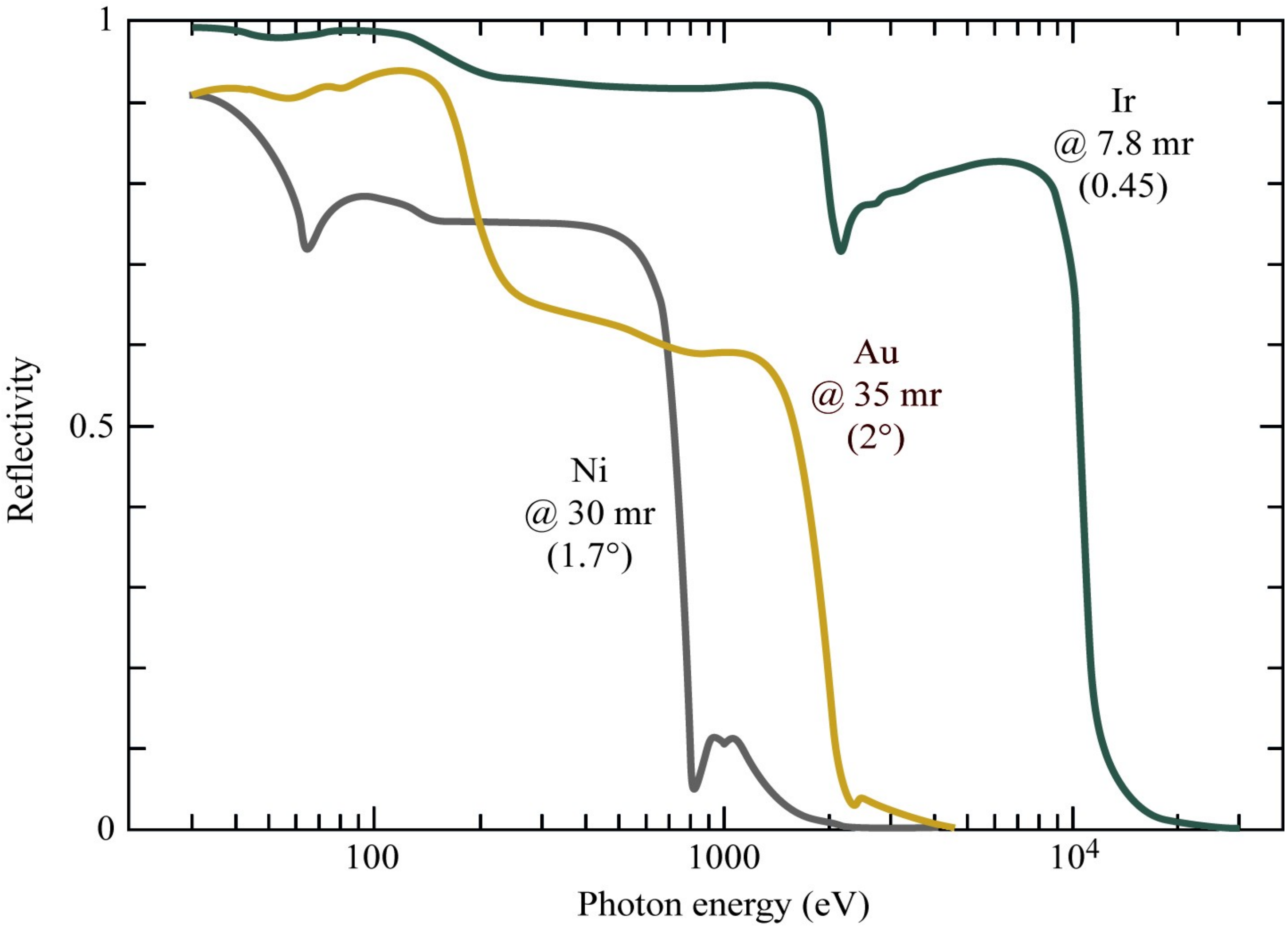

Courtesy of R. Soufli, LLNL, and E. Gullikson, LBL; www.cxro.LBL.gov/ical_constants

Two common zone plate x-ray microscopes

Full-Field Microscope

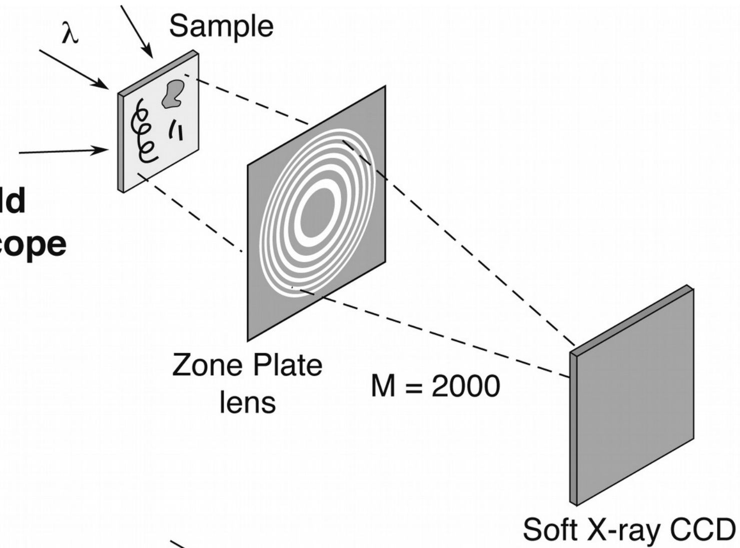

- 10–20 nm spatial resolution
- High spectral resolution
- Seconds exposure time
- Bending magnet, or undulator
- Higher radiation dose
- Flexible sample environment (wet, cryo, labeled magnetic fields, electric fields, cement, ...)

Scanning Microscope
(STXM)

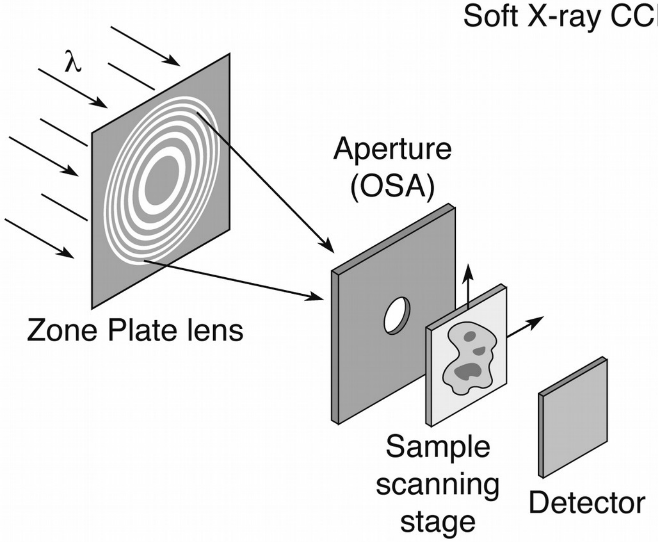

- 10–20 nm spatial resolution
- Least radiation dose
- High spectral resolution
- Requires spatially coherent radiation
- Minutes exposure time
- Flexible sample environment
- Photoemission, fluorescence imaging

Ch09_F21_Feb2017.ai

A Fresnel zone plate lens

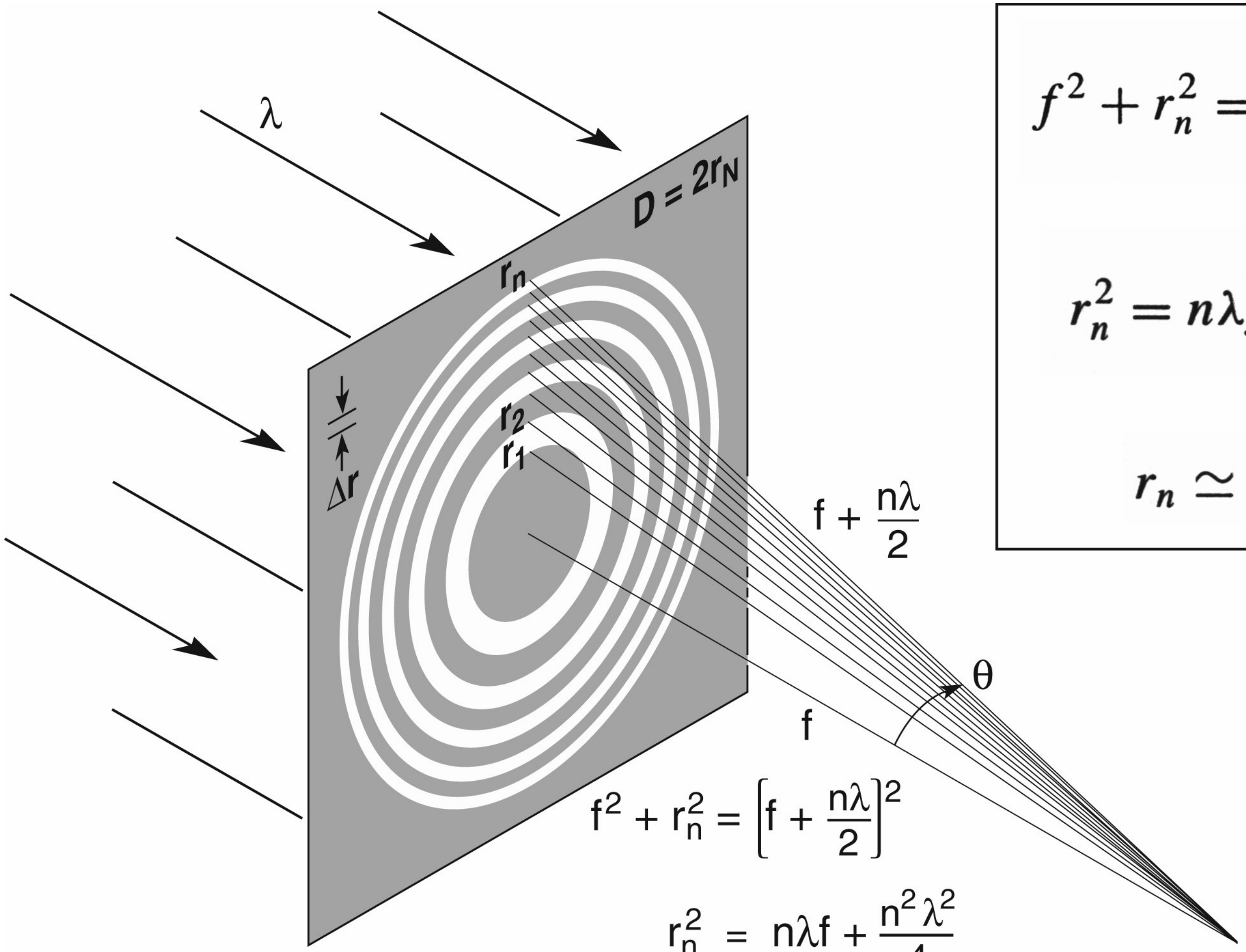

$$f^2 + r_n^2 = \left[f + \frac{n\lambda}{2}\right]^2$$

$$r_n^2 = n\lambda f + \frac{n^2\lambda^2}{4}$$

Ch09_F05VG.ai

$$f^2 + r_n^2 = \left(f + \frac{n\lambda}{2}\right)^2 \qquad (9.8)$$

$$r_n^2 = n\lambda f + \frac{n^2\lambda^2}{4} \qquad (9.9)$$

$$r_n \simeq \sqrt{n\lambda f} \qquad (9.10)$$

HW: Note right triangles. Use Pythagorean Theorem to derive zone plate equations above.

X-ray Fresnel zone plate lens can be used for imaging at high spatial resolution

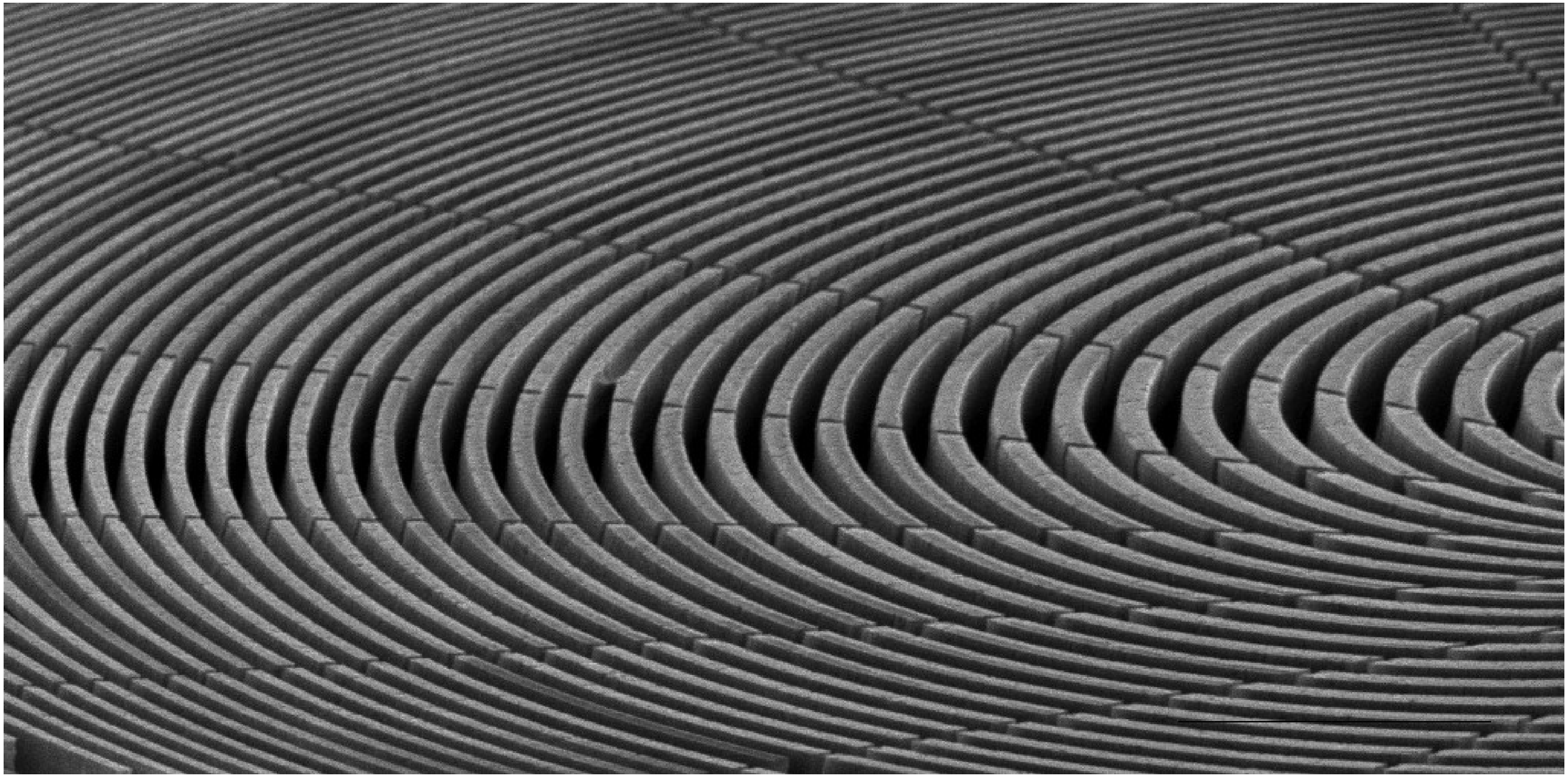

Courtesy of A. Sakdinawat and Chieh Chang (SLAC/ Stanford)

High resolution zone plate microscopy

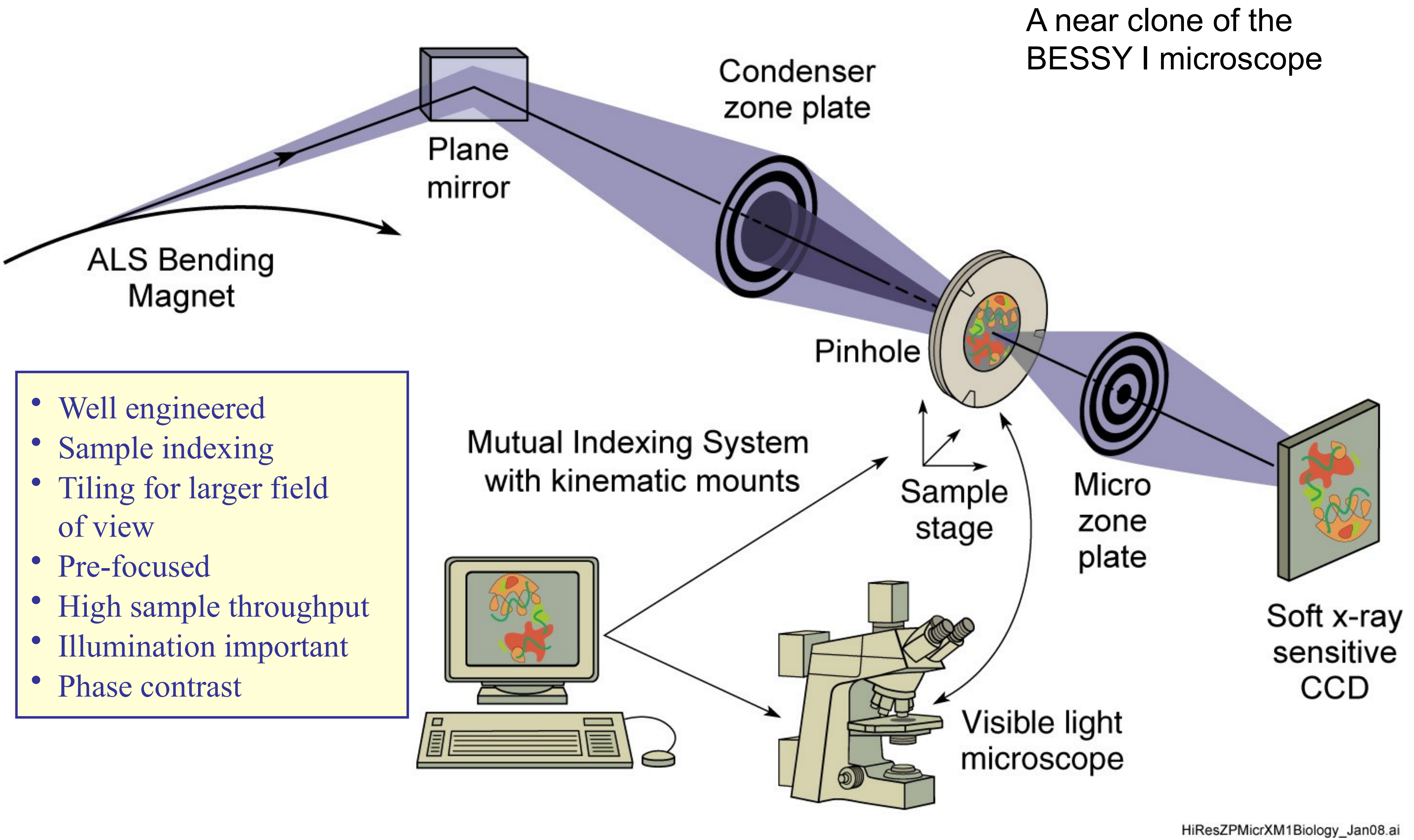

- Well engineered
- Sample indexing
- Tiling for larger field of view
- Pre-focused
- High sample throughput
- Illumination important
- Phase contrast

High resolution , 3D image of a mouse adenocarcinoma cell by soft x-ray tomography

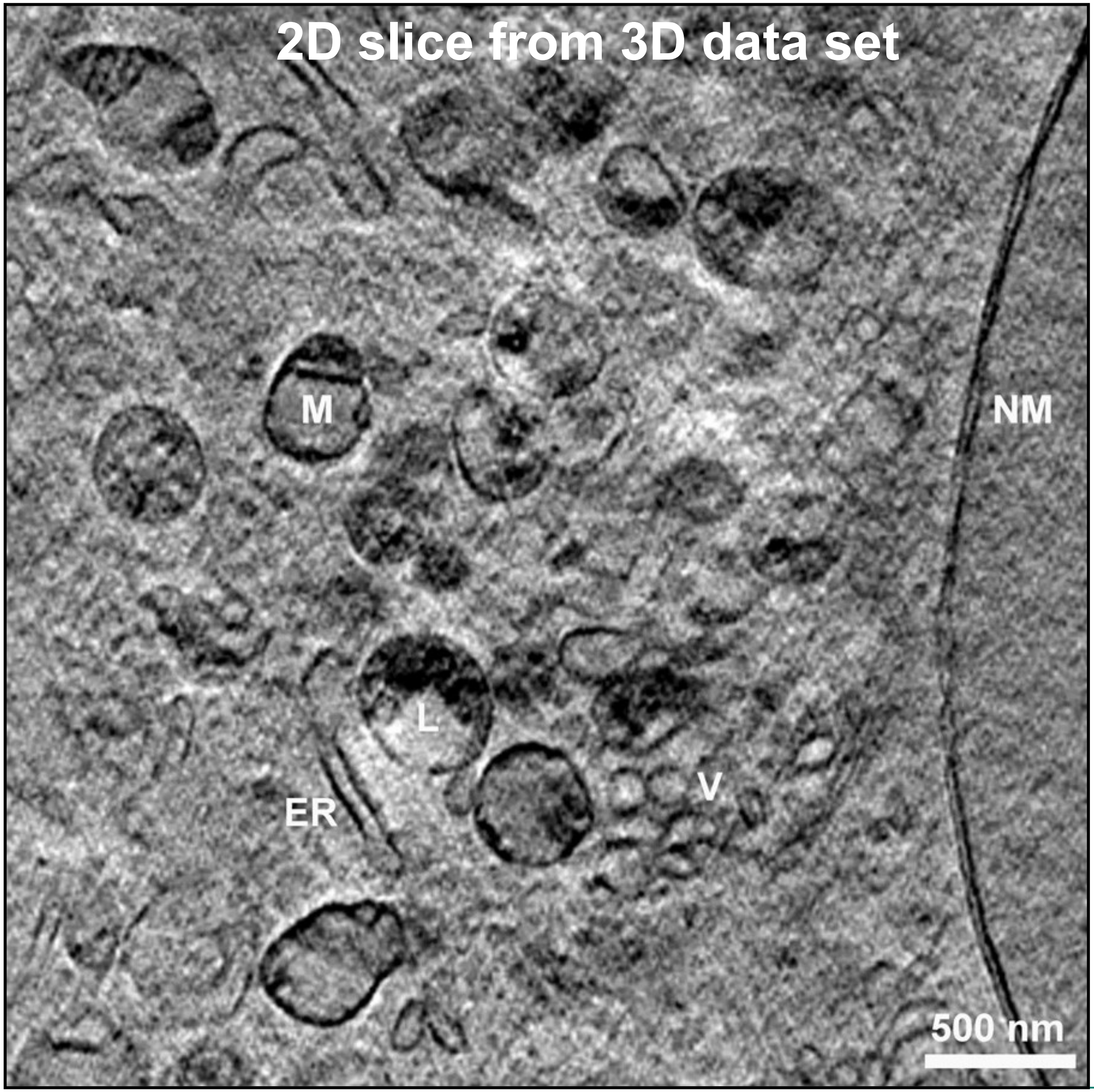

510 eV (2.43 nm)
Δr = 25 nm,
1° intervals, ±60°
36 nm nuclear double membrane.
Exposure ~ 5 minutes

Endoplasmic Reticulum (ER)
Mitochondria (M)
Nuclear Membrane (NM)
Lysosomes (L)
Vesicles (V)
Nuclear pores (NP)

Courtesy of Gerd Schneider, BESSYII and James McNally, NIH.
Nature Methods **7**, 985 (2010).

X-ray computed tomography of a single biological cell

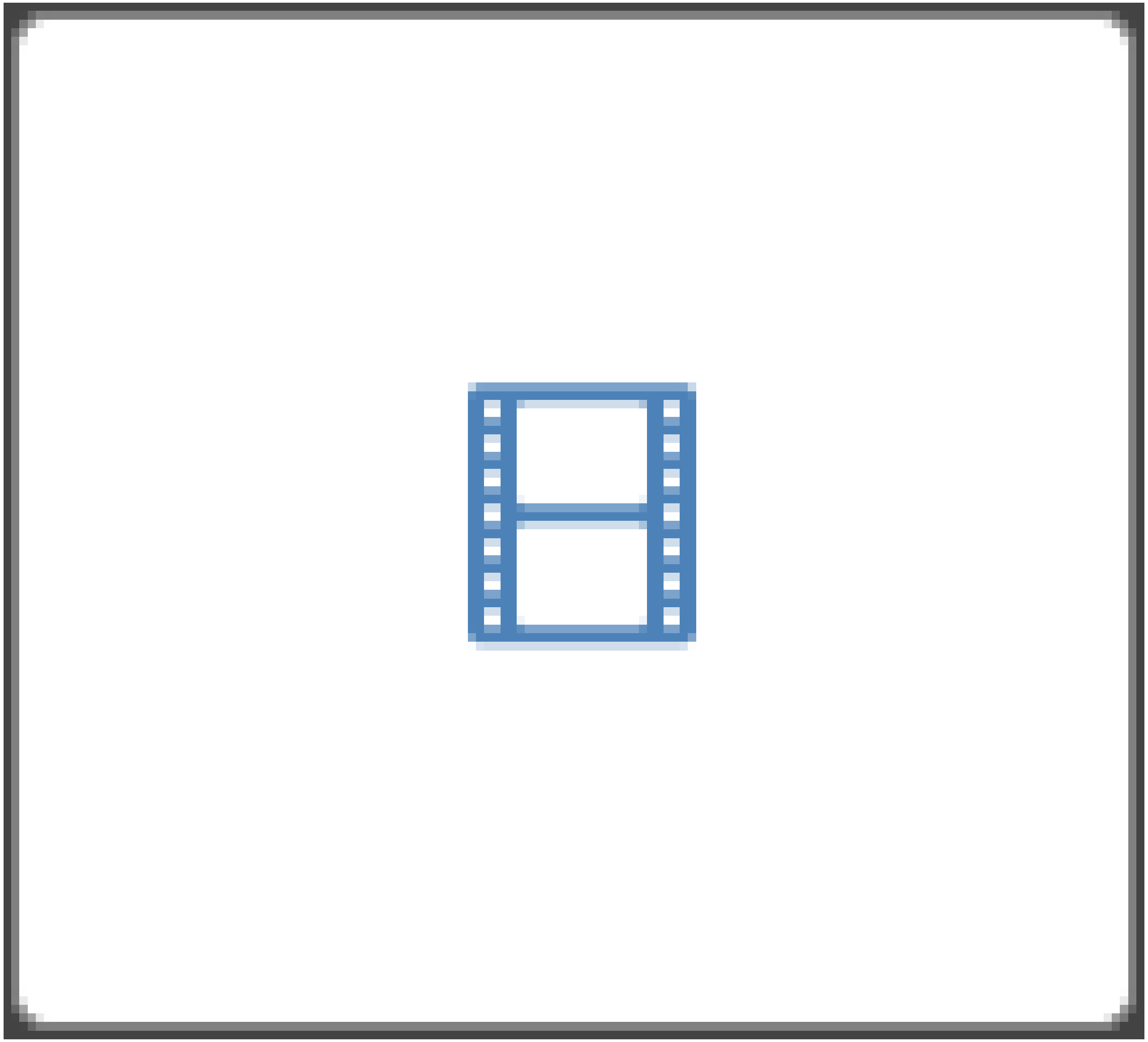

Courtesy of Gerd Schneider, BESSYII and James McNally, NIH.

Nano-spectroscopy of sodium titanate nanoribbons

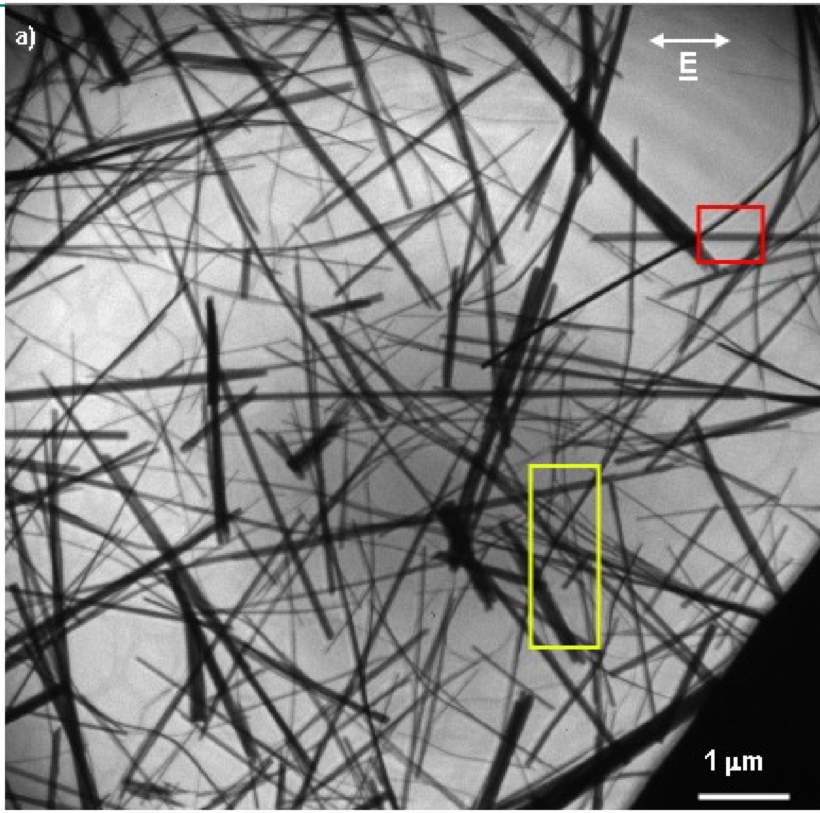

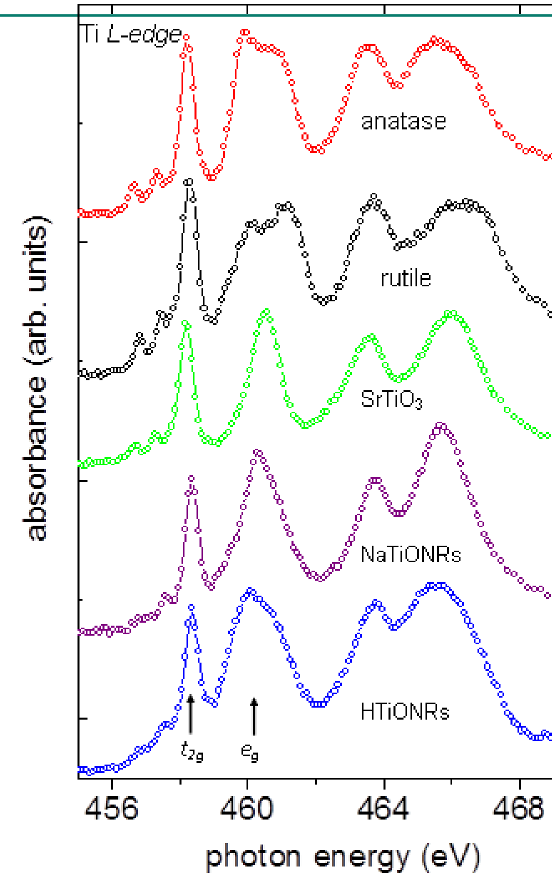

In collaboration with:
C. Bittencourt,
U. Antwerp, Belgium

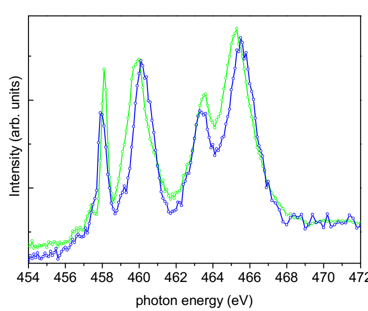

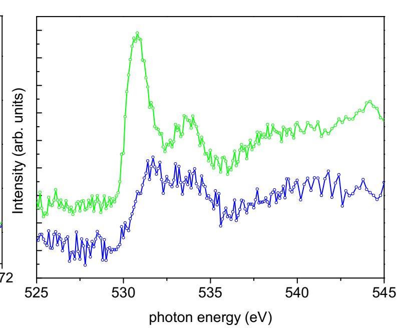

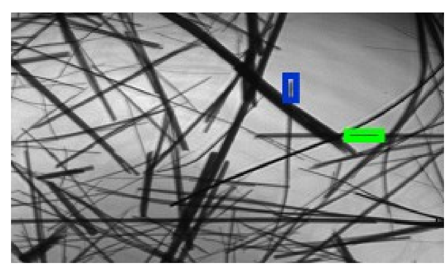

P. Guttmann et al., *Nature Photonics* (Dec. 2011).

Scanning Transmission X-ray Microscope (STXM)

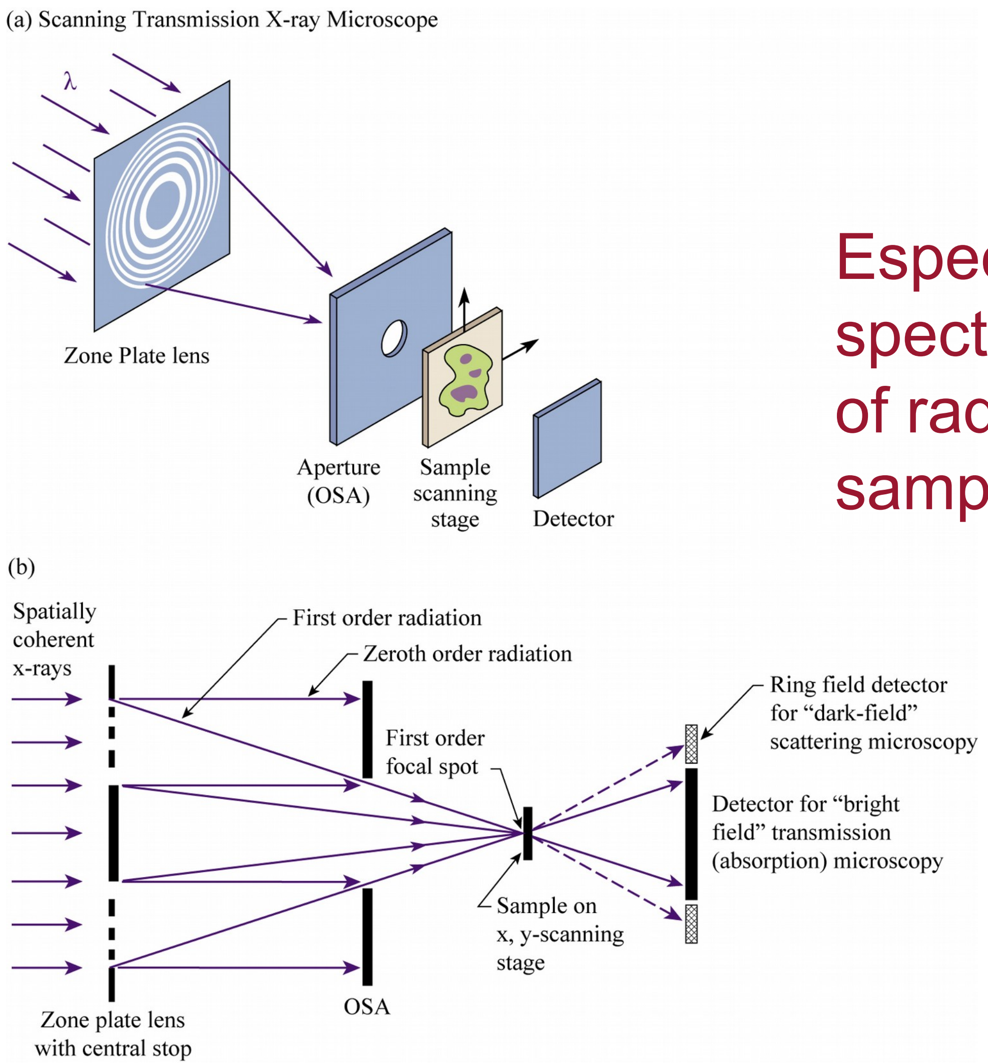

Especially useful for spectromicroscopy of radiation sensitive samples

Soft x-ray microscopy with 7 nm resolution

Scanning Transmission X-ray Microscope (STXM)
PSI, Swiss Light Source

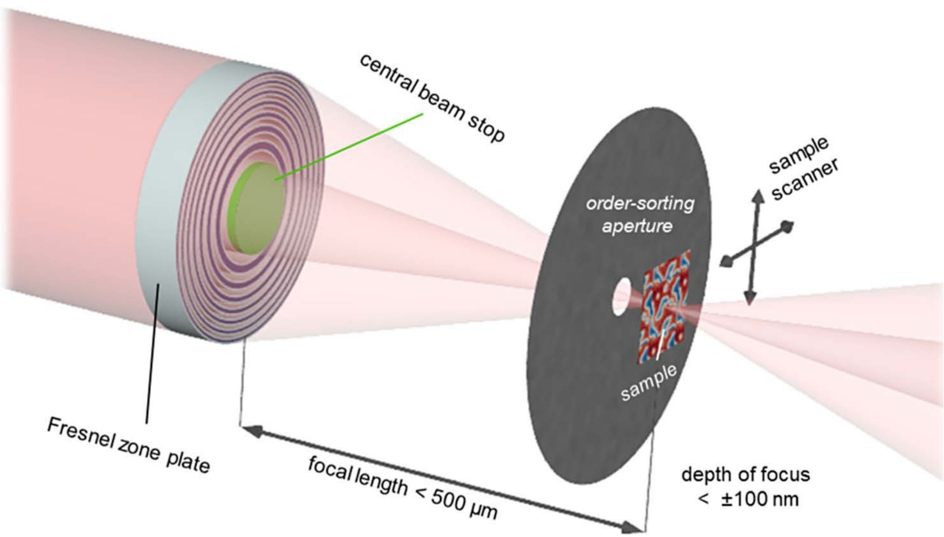

Magnetic nanostructure

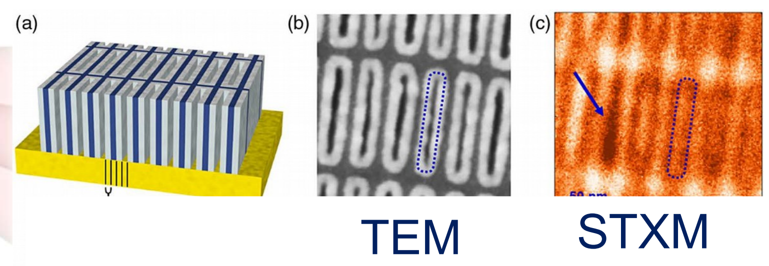

B. Rosner,* S. Finizio, F. Koch, F.Doring, V.A. Guzenko, M.Langer, E.Kirk, B. Watts, M.Meyer, J. Lorona Ornelas, A.Spath, S.Stanescu, S.Swaraj, R.Belkhou, T.Ishikawa, T.F. Keller, B.Gross, M.Poggio, R.H.Fink, J. Raabe, A. Kleibert, AND Christian David **Optica** 7, 1602 (November 2020).

PSI, ETH, Erlangen-Nurnberg, Soleil, DESY. U.Hamburg, U.Basel

Environmental study: Biofilm from Saskatoon River

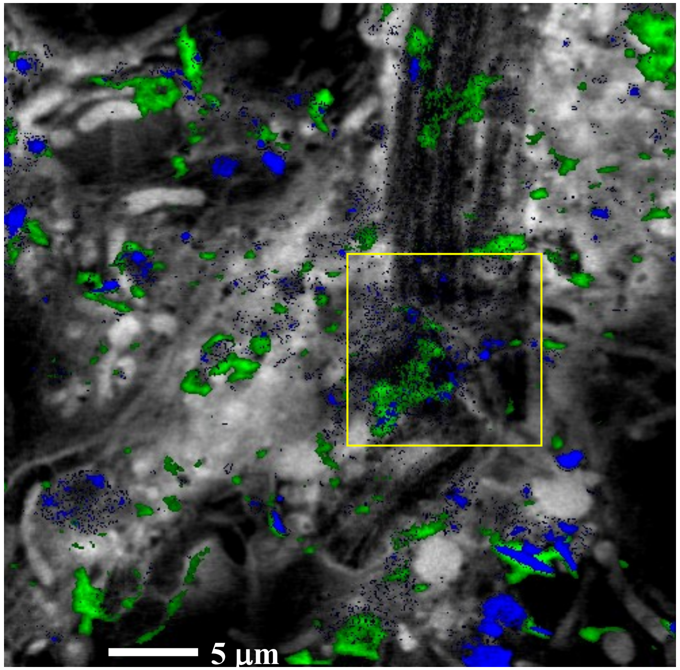

Protein (gray), Ca, K

RESULTS

- Ni, Fe, Mn, Ca, K, O, C elemental map, (there was no sign of Cr.)
- Different oxidation states for Fe and Ni

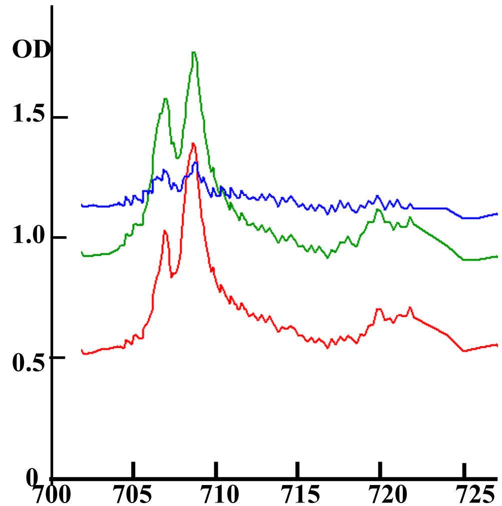

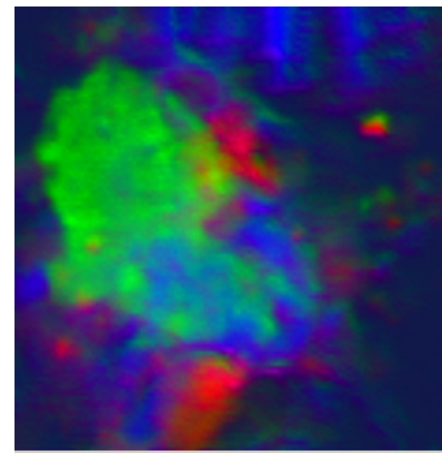

Different oxidation states (minerals) found for Fe & Ni

Courtesy of Tohru Araki, Adam Hitchcock (McMaster University) and Tolek Tyliszczak, LBNL;Sample from: John Lawrence, George Swerhone (NWRI-Saskatoon) and Gary Leppard (NWRI-CCIW)

A High Quality Mo/Si Multilayer Mirror can Achieve 70% Normal Incidence Reflectivity in the EUV

Small reflections at many interfaces add in phase at the Bragg angle.
In the EUV δ and β are relatively large (dependence)

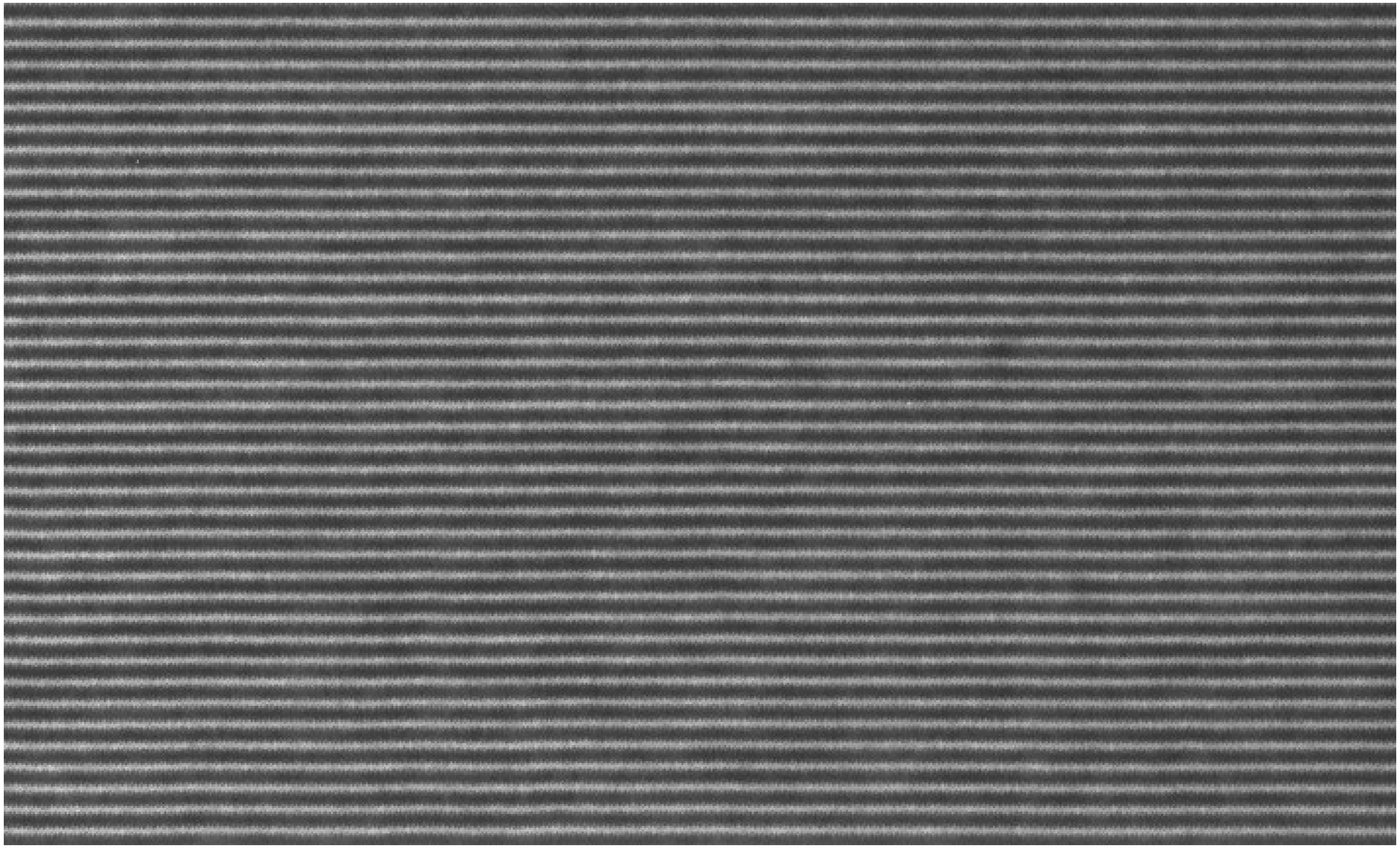

N = 40
d = 6.7
λ = 13.5 nm
(92.5 eV)

Courtesy of Šaa Bajt (CFEL/DESY)

Multilayer mirrors have achieved a reflectivity of 70% in the extreme ultraviolet (EUV) … an unusual result

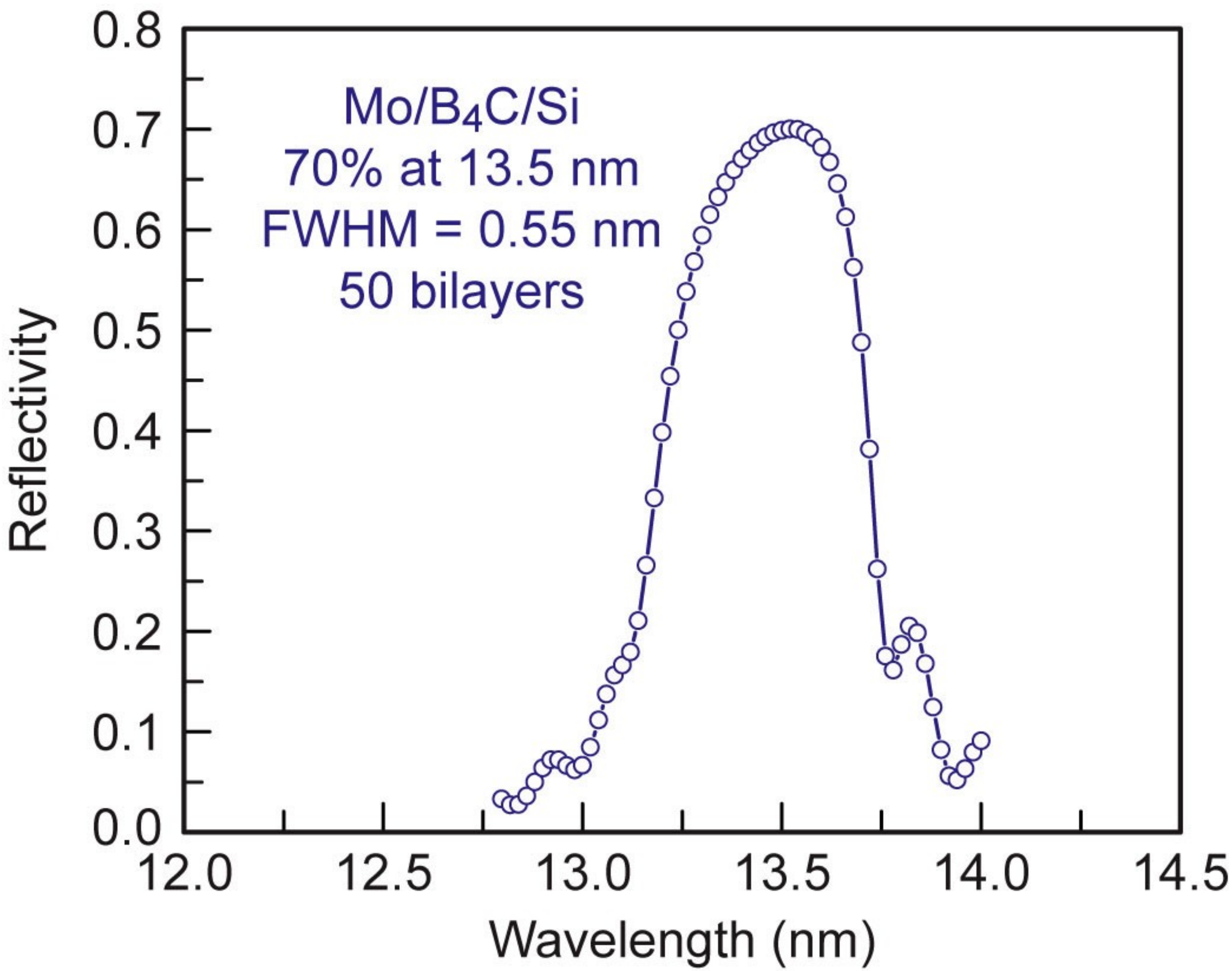

Courtesy of Saša Bajt (LLNL)

Ch04_ReflectCurv70.ai

EUV Image obtained with Mo/Si coated optics: coronal loop of magnetized plasma at the sun's surface

Lockheed/NASA Atmospheric Imaging Assembly (AIA) telescope, part of the geo-synchronous Solar Dynamics Observatory (SDO).

Multilayer coatings provided by R. Soufli, LLNL and D.L. Windt, Reflective X-ray Optics. J.R. Lemen, Solar Physics **275**,14 (2012)

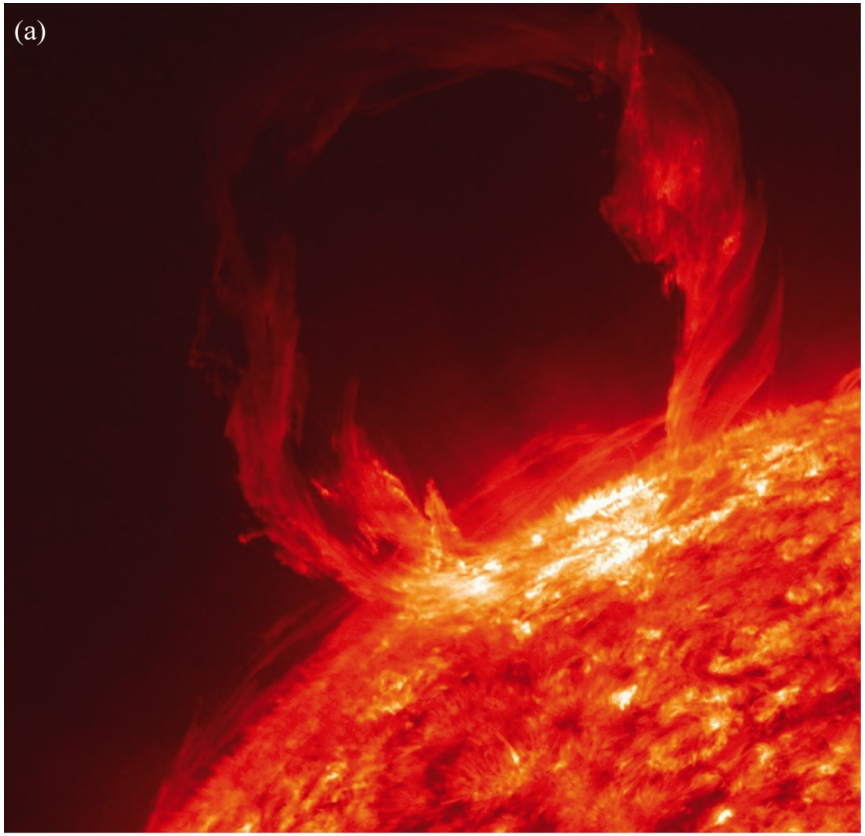

NASA/SDO

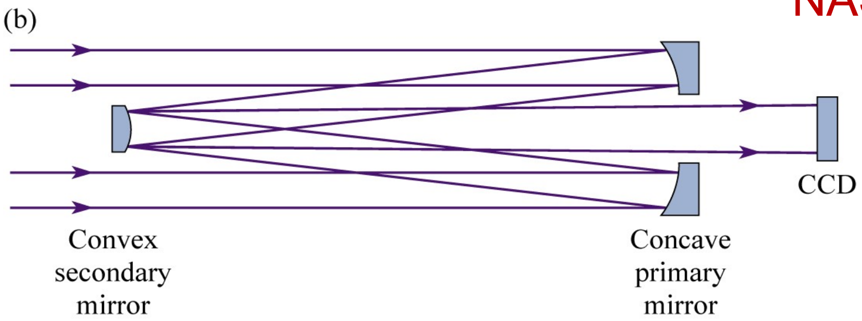

Multilayer coated Cassegrain telescope Mo/Si, 17.1 nm,

Moore's Law is not dead, saved by Extreme Ultraviolet (EUV) Lithography using these same multilayer mirrors

Step and scan system, Mo/Si coated reflective optics at 13.5 nm wavelength, CO_2 laser irradiated 30 μm Sn microspheres.

Bending magnet and undulator radiation used for critical early research at both the ALS and BESSY II.

Courtesy of V. Banine (ASML) and W. Kaiser (Zeiss)

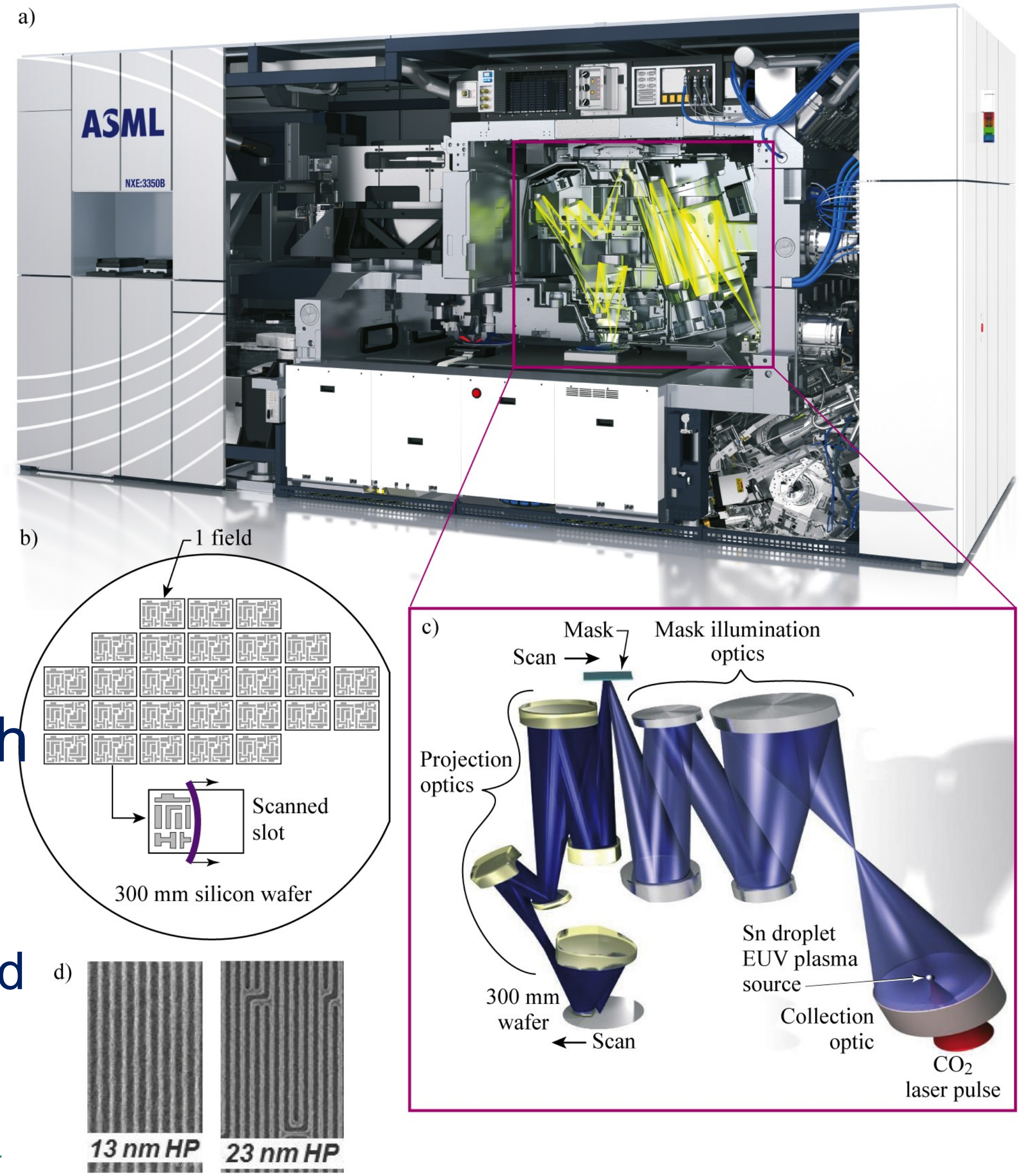

EUV lithography: High volume manufacturing (HVM) of computer chips and smart phone chip began in 2019

ANANDTECH
9 October 2018

TSMC's second-generation 7 nm manufacturing technology will use extreme ultraviolet lithography.

Apple's new iPhone 11 uses TSMC chips patterned by EUV lithography

VB VentureBeat
18 October 2018

Samsung begins making 7LPP chips, commercializing 7nm EUV lithography

7nm EUV lithography In a significant milestone for the semiconductor industry, Samsung today announced that it is now manufacturing 7LPP chips: processors based on extreme ultraviolet lithography (EUV) and a 7-nanometer manufacturing process. Beyond this specific accomplishment, the company notes that it is providing customers a clear path to future 3-nanometer chips.

Further reading, 2021 online lectures, slides that you can use

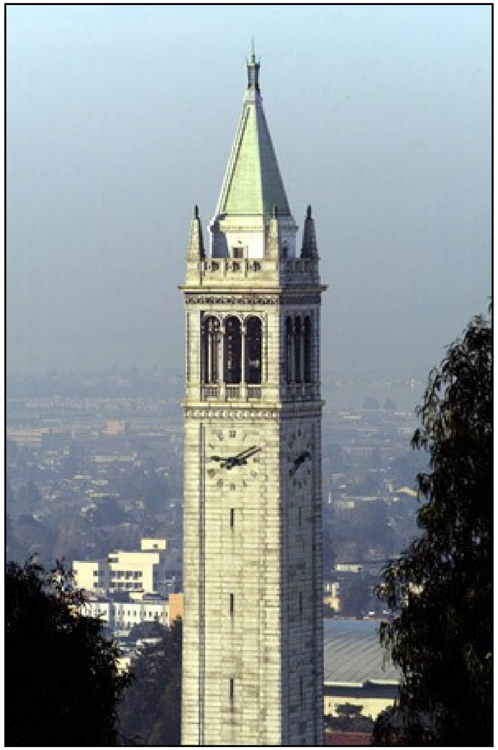

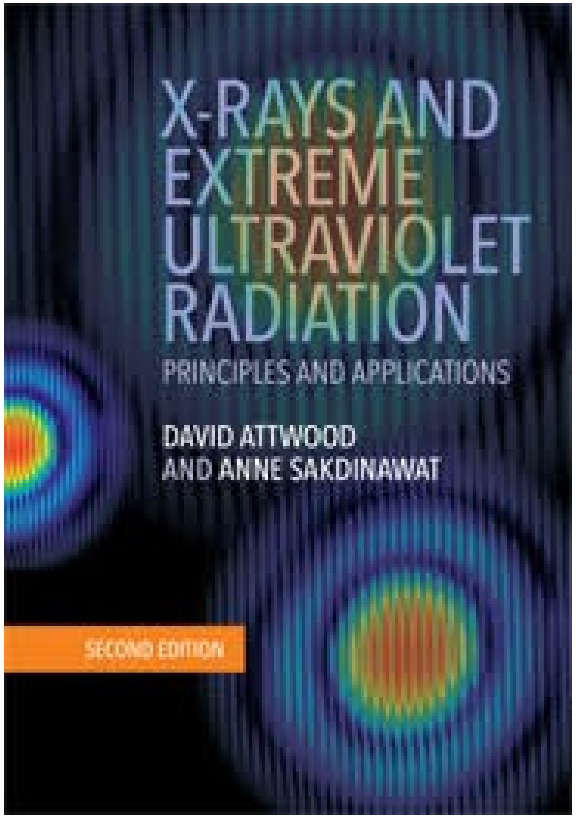

UC Berkeley 2021 lectures online:
https://www.youtube.com/playlist?list=PL2wgq6z751n6EIeNsPAx_b8eIkmLS41GT

Cambridge University Press
www.cambridge.org/xrayeuv
For slides, errata and HWs click 'Resources'